AN INVESTIGATION OF BANDING IN STEEL BY SIMULATION

AN INVESTIGATION OF BANDING IN STEEL BY SIMULATION

by

JULIUS VON DESTINON-FORSTMANN, B.Sc.

A Thesis

Submitted to the Faculty of Graduate Studies

in Partial Fulfilment of the Requirements

for the Degree

Master of Science

McMaster University

May 1961

MASTER OF SCIENCE
(Metallurgy)

McMASTER UNIVERSITY
Hamilton, Ontario.

TITLE: An Investigation of Banding in Steel by Simulation

AUTHOR: Julius von Destinon-Forstmann, B.Sc. (McMaster University)

SUPERVISOR: Dr. J.S. Kirkaldy.

NUMBER OF PAGES: viii, 48.

SCOPE AND CONTENTS:

This thesis describes a study of the fundamental aspects of banding in steel. The banded structure is simulated by means of layer diffusion couples. Consideration is given to the amount of carbon presegregation that occurs in the austenitic state due to activity differences arising from a non-uniform distribution of alloying elements as well as to the segregation which occurs during subsequent transformation. A new method for the experimental determination of the off-diagonal diffusion coefficients which control the presegregation in ternary systems is described. Different cooling rates are used to investigate the contribution of transformation segregation toward the final structure. The effect of cooling rates on the final structure is investigated metallographically.

PREFACE

This work was undertaken to investigate the various factors involved in banding in steels. Towards this end,

a) a new experimental method was developed for simulating banding and determining transient equilibrium concentrations of carbon in iron in the presence of alloying elements.

b) a quantitative study was undertaken to determine the amount of presegregation which occurs in iron-carbon/iron-chromium-carbon, iron-carbon/iron-manganese-carbon, iron-carbon/iron-phosphorus-carbon, and iron-carbon/iron-silicon-carbon diffusion couples over the range of temperatures 930°C to 1100°C.

c) a metallographic investigation was carried out to determine the transformation segregation contribution to banding with cooling rates varying between 1.2°C/min and 50°C/min.

ACKNOWLEDGMENTS

The author is indebted to Dr. J.S. Kirkaldy for suggesting the problem and for his advice and encouragement during the course of this work. I would also like to acknowledge the financial assistance made through the annual grant from the American Iron and Steel Institute to Dr. J.S. Kirkaldy. I am grateful to Mr. John Kelly of the Steel Company of Canada for assisting with some of the analyses, to Dr. H.I. Aaronson of Ford Motor Company for providing the plain carbon steels used, to Mr. G.R. Purdy of the McMaster University Department of Metallurgy for assistance and advice and to the staff of the McMaster Engineering Building for continued technical assistance.

TABLE OF CONTENTS

LIST OF ILLUSTRATIONS

LIST OF TABLES

I

INTRODUCTION

More than ever before, technological advances demand the ultimate in utilization of the available properties of materials. An investigation into the basic factors involved in banding in steels is of great technical importance since in the elimination of banding lies a possible increase in the physical properties of steels.

Ever since the early days of metallography it had been noted that steels after mechanical deformation by rolling or forging exhibited a layer-like structure of nearly parallel bands aligned in the direction of working. This was termed a banded structure and a typical example is shown in Fig. 1.

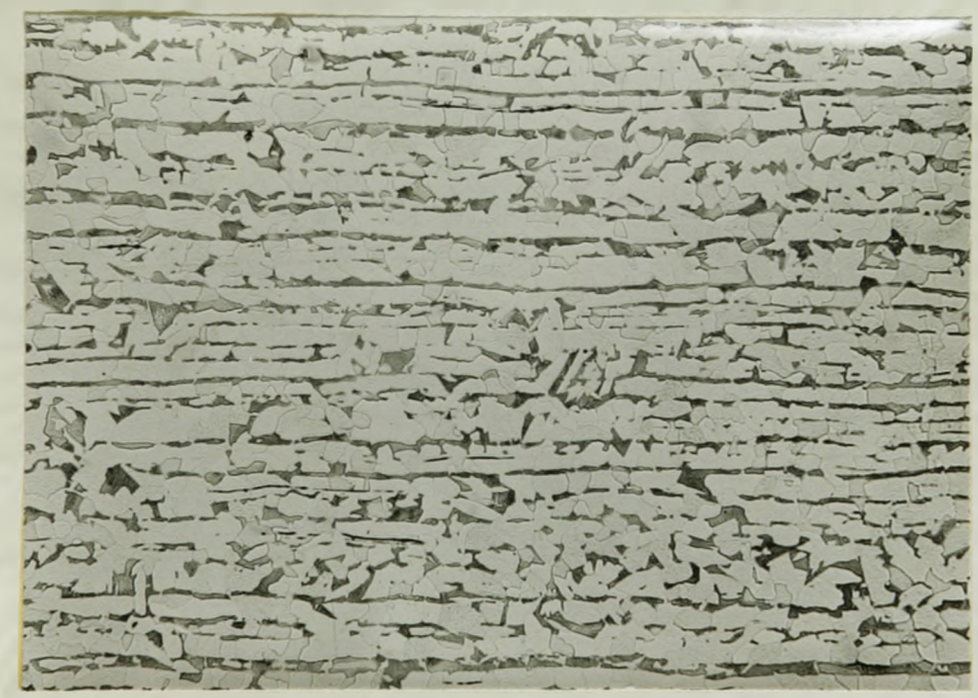

Fig. 1. Photomicrograph of typical commerical banded steel.

The banded structure shown in Fig. 1 is sometimes referred to as "Ghost Lines" and consists of layers or bands of ferrite and pearlite. Even in the early days of metallography the relative mechanical properties of ferrite compared to pearlite were known and the directionality of banded structures was recognized, and ever since, technology has worked towards reducing or eliminating banded structures. Unfortunately, to this day, little practical progress has been made, although it is evident from the literature published on the subject that great efforts have been made to elucidate the problem.

A SURVEY OF THE LITERATURE ON BANDING

All previous investigations of banding have been carried out with commercial steels. Lavender and Jones[1], studied banding by micro-radiography in chromium, manganese and molybdenum steels. They proved conclusively that these elements segregate on freezing and are aligned into persistent bands by subsequent working. These banded steels were given solution treatment at various times and temperatures. The temperatures required to remove banding were found to be of the order of 1200° - 1300°C which was in agreement with rough calculations based on diffusion data and the width of the bands present. They pointed out that solution treatment at these temperatures would likely result in overheating of commercial steels. The high temperatures which are reported by Lavender and Jones as necessary to remove manganese segregation are in disagreement with the results reported by Wolfe[2] in the discussion of Betteridge and Sharpe's[3] paper.

The results obtained by Lavender and Jones are substantiated by

Schwarzbarts[4] paper on the effect of manganese banding on the mechanical properties of heat treated steel plate. Schwartzbart, with solution treatment of manganese steels for 6 hours at 1245°C, increased the strength by 10% and ductility by a factor of from 2.5 to 8.5. His procedure consisted of quenching his samples after the solution treatment and tempering them between 100° and 600°C. He reasoned that since transformation is a nucleation and growth process and is therefore diffusion dependent he would, by quenching, eliminate the segregation of carbon which occurs on transformation, and thus eliminate banding. As pointed out by Jatczak et al[5], this is only partially correct. The fault in the argument lies in the assumption that a specimen which has a banded distribution of manganese will have a uniform distribution of carbon in the austenitic region.

Jatczak et al arrived at the following conclusions. The primary cause of banding in rolled steel products is chemical heterogeneity, which produces visible banding through its effects on nucleation and growth of ferrite and pearlite from austenite. The pattern of nucleation and growth of ferrite and pearlite is determined primarily by the effect of alloy heterogeneity on carbon segregation. They demonstrated the persistence of this heterogeneity by taking the sluggishly transforming commercial 4340 steel, quenching it to the nose of its TTT curve and allowing an incubation period of various times as shown in Fig. 2. They found that ferrite and pearlite were nucleated and grew into bands even after prior homogenization treatments of 50 hours at 1204°C. They were led to this experiment on finding that a direct quench to the martensitic structure did not show any banding after homogenization for only 5 hours at 1204°C, in disagreement with estimates of homogenization times based on diffusion data for the alloying elements concerned.

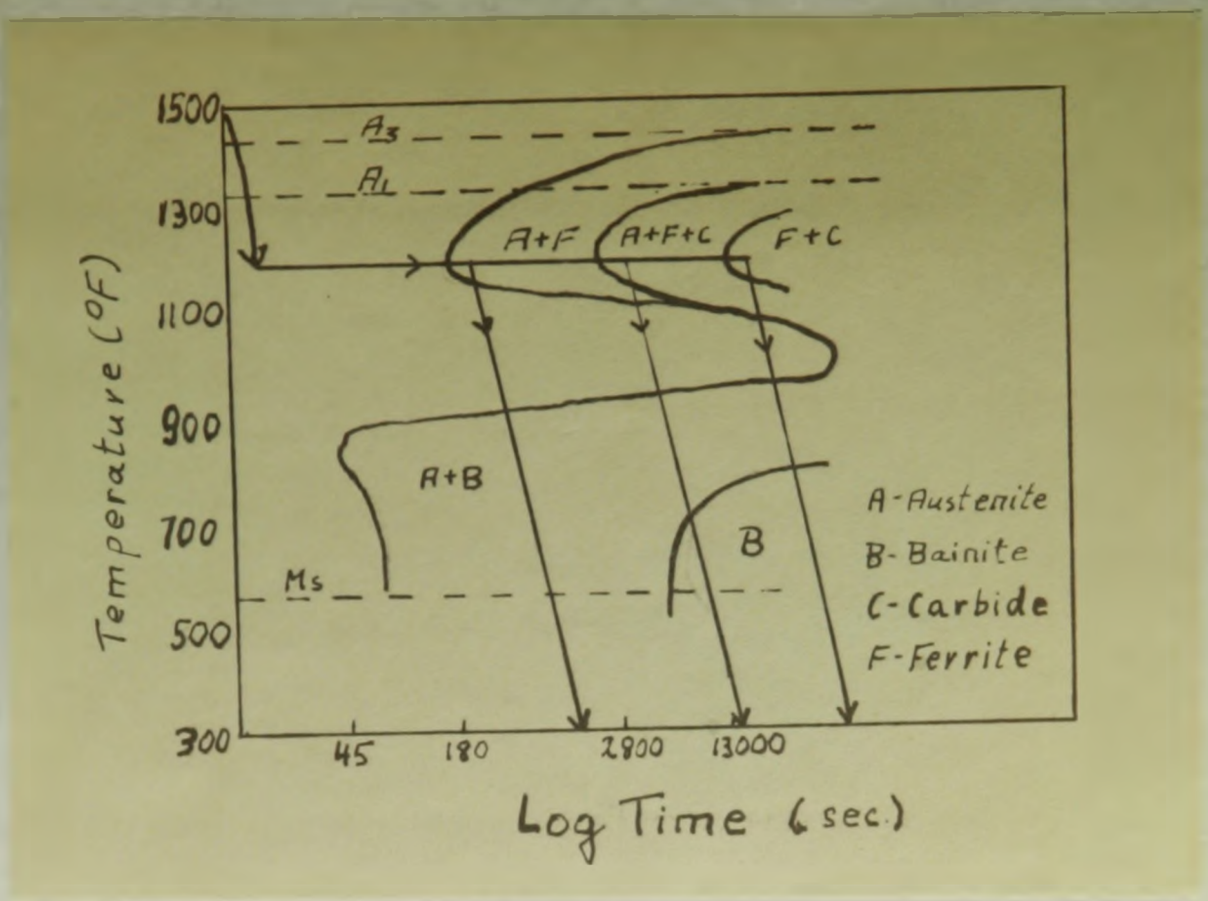

Fig. 2. Thermal schedules employed in the study of banded 4340 steel superposed on the time-temperature-transformation curve (after Jatczak et al[5])

The same investigators concluded that carbide-forming elements tend to lower the activity of carbon in the alloy rich regions while solution-type elements like nickel tend to increase the activity of carbon in their vicinity. They arrived at this conclusion by observing the sulfide inclusions, which are always found in the interdendritic, alloy-rich regions. These appeared in the high carbon (pearlitic) regions for the carbide-forming elements, and in the low carbon (ferritic) regions for the solution-type elements.

Similar experiments were carried out by Ploeckinger and Randak[6]. They investigated the amount of banding in commercial steels after different homogenization times and temperatures and different cooling schedules.

The metallographic techniques used in this investigation are notable. By etching the lower half of the polished samples in Oberhoffer's reagent* and the upper half in notal+ they were able to locate the alloy segregation and the distribution of carbon with respect to it.

The quantitative results disagree with those of Jatczak et al in that after solution treatment for 30 hours at 1150°C no more banding could be detected, even on cooling at the rate of 0.4°C/min. The fundamental value of the paper is limited since the alloys used were aggregates of many elements with competing effects on banding. Their paper does show, however, the need for recognition of the basic factors controlling banding.

The Hatfield Memorial Lecture, given by Bastien[7], on the mechanism of formation of banded structures is less noteworthy for its experimental findings than for its theoretical considerations. Bastien was the first to enumerate all the metallurgical factors involved in the formation of banded structures. He distinguished between large scale segregation, defined as the variation in concentration between the liquid and solid phases which are found over the entire ingot, and dendritic segregation, which affects the crystals of primary crystallization and depends on the existence of solid solutions in which the concentration varies with temperature. He particularly realized that the metallurgical history of the

---

* Oberhoffers reagent is a solution of cupric chloride in ethyl alcohol. The etch reveals highly alloyed areas.

\+ Nital is a dilute solution of nitric acid and ethanol. It reveals pearlitic areas and grain boundaries in plain carbon and low alloy steels.

material used for investigation played the dominant role in the intensity of the banding produced. The mechanism which he proposed for the formation of a banded structure was developed on the basis of phosphorus segregation in a hypoeutectoid low carbon steel.

Bastien starts with the proposition that after solidification there will be more carbon and phosphorus atoms in the interdendritic spaces than near the axes of the dendrites and that this segregation will effect the local constitution of the steel. Fig. 3 shows the influence of phosphorus on the A_{c3} and A_{c1} lines as established by differential dilatometry in a 0.28% carbon, 1.56% nickel, 0.52% chromium, commercial steel.

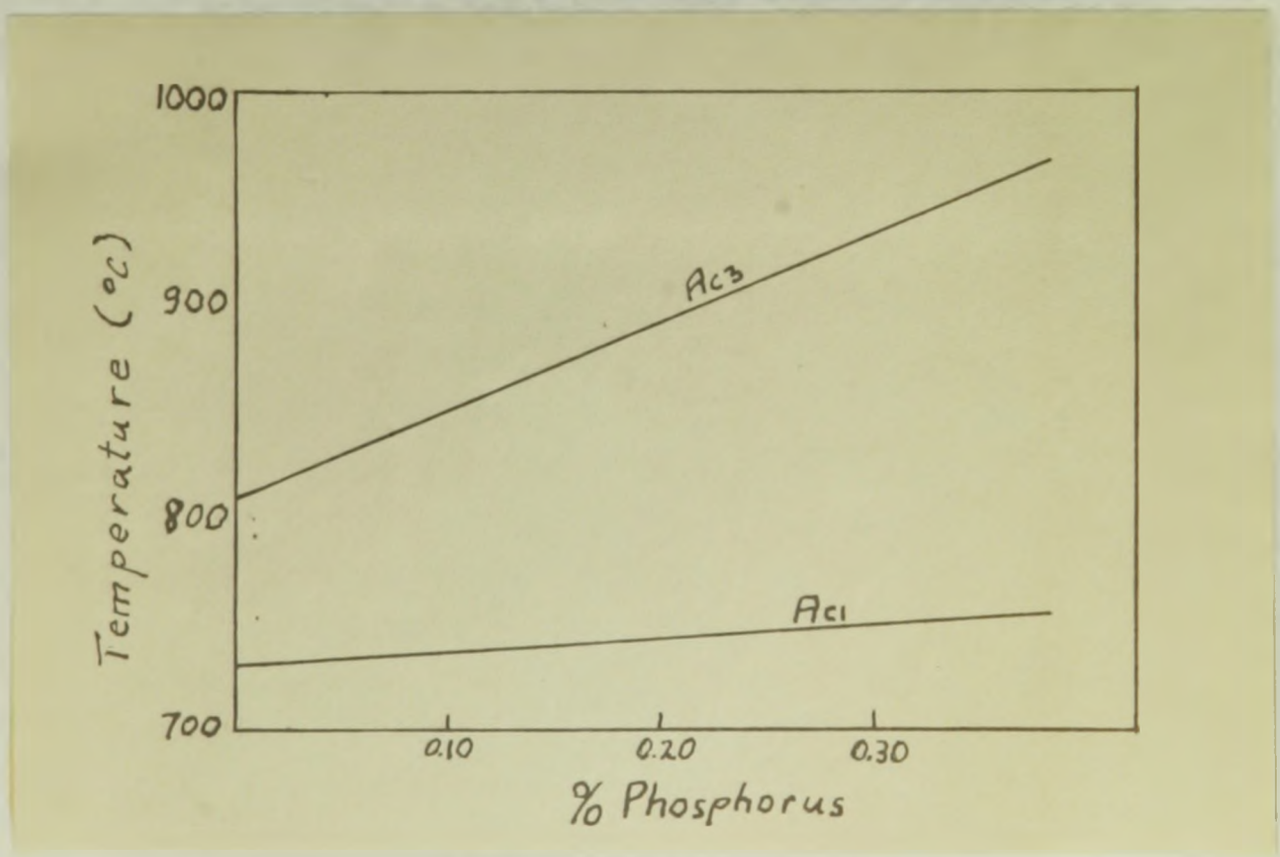

Fig. 3. Influence of Phosphorus on the A_{c1} and A_{c3} points of a 0.28% carbon, 1.56% nickel, 0.52 chromium steel (after Bastien[7].)

During cooling which is slow enough to allow the austenite to transform in the upper range of the TTT curve the areas with high phosphorus content will tend to become ferritic at a higher temperature than the areas with low phosphorus, while the carbon will become concentrated in those regions which are still austenitic. Carbon, and not phosphorus, diffuses from the areas high in phosphorus even if it has to diffuse uphill, i.e., into areas of already high carbon concentration. This is possible because diffusion is controlled by activity and not concentration gradients. Thus, carbon diffuses from an area of high activity to an area of low activity.

According to Grossman[8] phosphorus also produces a relatively large increase in the hardenability of steel. Thus, if there is both a rise in the A_3 transformation temperature and an increase in the hardenability, the TTT curves representing the start of the austenite transformation in areas of different phosphorus content must intersect, as shown in Fig. 4.

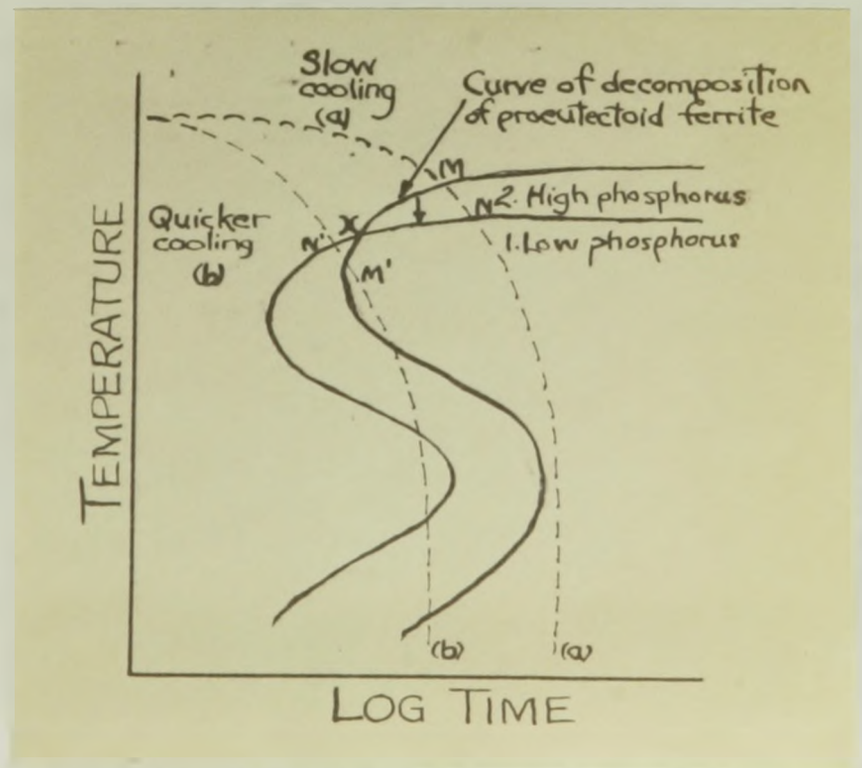

Fig. 4. Time-temperature-transformation (TTT) diagram showing conditions for reversal of carbon migration in phosphorus steels (after Bastien[7]).

Curve (1) corresponds to the dendrite axes while (2) corresponds to the alloy-rich interdendritic areas. If cooling takes place slowly (curve a) the cooling curve would intersect curve (2) at M and curve (1) at N which is at a lower temperature. Ferrite would first deposit in regions with a higher phosphorus content resulting in concentration of carbon in the remaining austenite. With a more rapid rate of cooling the corresponding cooling curve (b) intersects the transformation curves (1) and (2) at N' and M' respectively. The austenite transformation now begins in regions with the low phosphorus content, tending to produce a concentration of carbon in areas rich in phosphorus. The usual carbon migration away from phosphorus rich areas will therefore not take place.

This conception lead Bastien to the conclusion that for a steel of suitable composition there exist cooling rates that could reverse the carbon distribution normally obtained. Thus, by suitable heat treatment, carbon banding could be eliminated. He realized, however, that the increase in hardenability due to phosphorus in the usual commercial quantities was not large enough to be of practical value.

On surveying the literature it was felt that the complexity of the problem recommends against the use of commercial steels in an investigation on banding. This is because such steels contain alloying elements with competing and ambiguous influence on the banded structure. For this reason pure base materials were used throughout in preparation of the ternary alloy systems to be studied experimentally. It was further recognized that a clear distinction has to be made between the two prime contributors to banding; carbon presegregation (which was emphasized by Jatzek et al [5]) and segregation during transformation (which was emphasized by Bastien [7]).

THEORETICAL CONSIDERATIONS IN BANDING.

In this thesis segregation is defined as the difference of alloy concentration between an enriched area and an adjacent area which is depleted in this alloying element. In particular, this could be the difference between the alloy content of an interdendritic area and the alloy content of the adjacent dendrite core. Banding is the alignment of this segregated structure into parallel bands by unidirectional mechanical deformation. Confining our discussion to carbon banding only, which is manifested in the final microstructure by pearlite layers, we find this condition is the result of two distinct processes:

1) Presegregation, which is the segregation of highly mobile carbon which occurs in the austenite range prior to transformation. This is a result of the tendency to equalize carbon activities in the presence of a sluggish distribution of other alloying elements.

2) Transformation segregation, which is the re-distribution of carbon occuring during transformation of the austenite solid solution through the A_3 to A_1 region of the equilibrium diagram.

When alloys solidify, the transformation structures obtained are very far from the equilibrium structures predicted by the phase diagram due to the sluggishness of diffusion in the solid dendrites as solidification proceeds. Hayes and Chipman[9] first calculated the non-equilibrium distribution of solute in a solidifying binary alloy on the assumption that solid state diffusion is negligibly small while the liquid diffusion rate is sufficiently fast to maintain the liquid solute distribution uniform.

Consider the schematic binary phase diagram of Fig. 5, and the solidification of an alloy of concentration C_o.

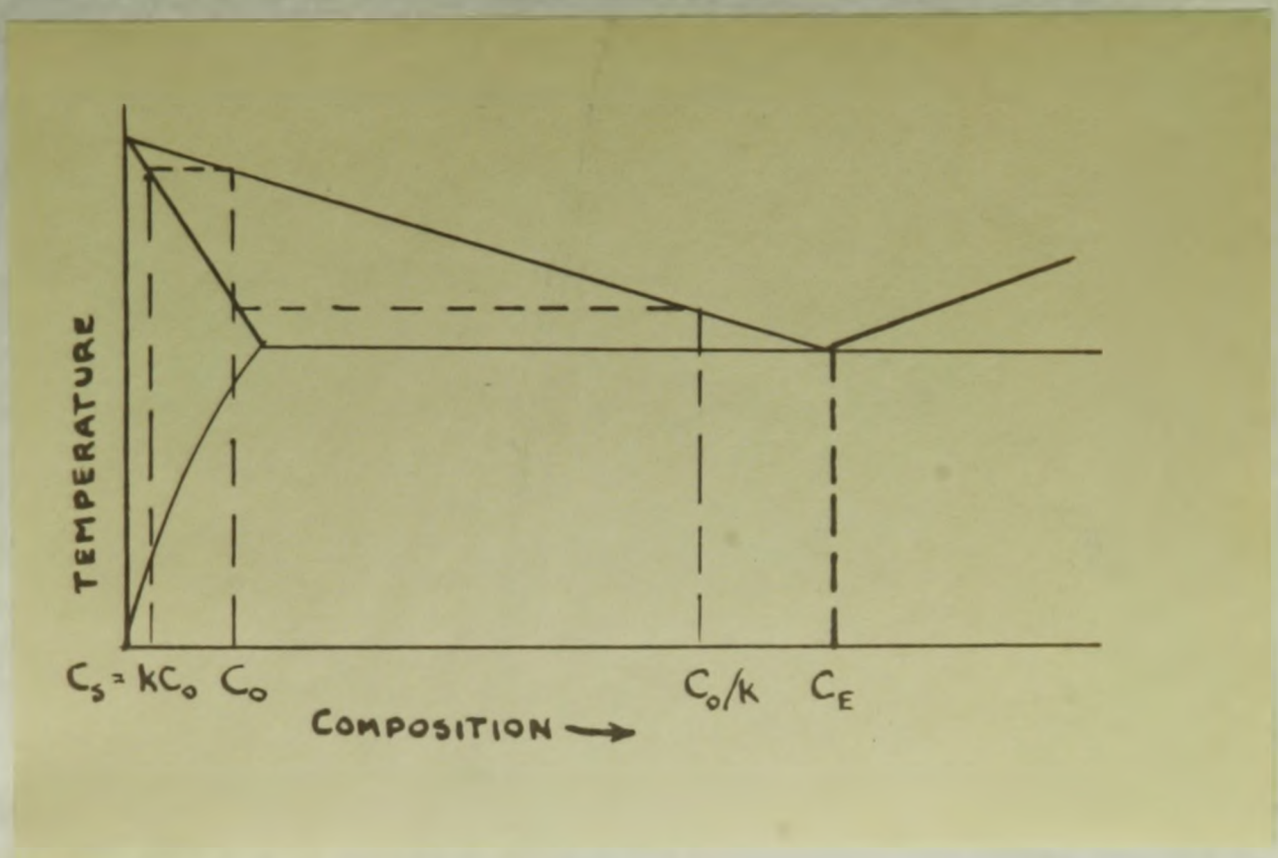

Fig. 5. Schematic phase diagram used in segregation calculations.

At equilibrium the first solid to appear would have a concentration kC_o, where k is the so-called distribution coefficient, while the last liquid existing in the system would have concentration C_o/k. In the non-equilibrium model introduced above, the solute distribution as it varies from a dendrite core to the interdendritic median at some time t is given in Fig. 6, according to the assumption that no diffusion has occurred in the solid while an infinite diffusion rate in the liquid maintains a uniform liquid distribution. Consider an incremental amount of solidification measured by a decrease in the mass of liquid dm_L corresponding to an increase in liquid concentration dC_L. Since solute must be conserved,

$$-(C_L - C_s)\, dm_L = m_L\, dC_L = -C_L\,(1 - k)\, dm_L.$$

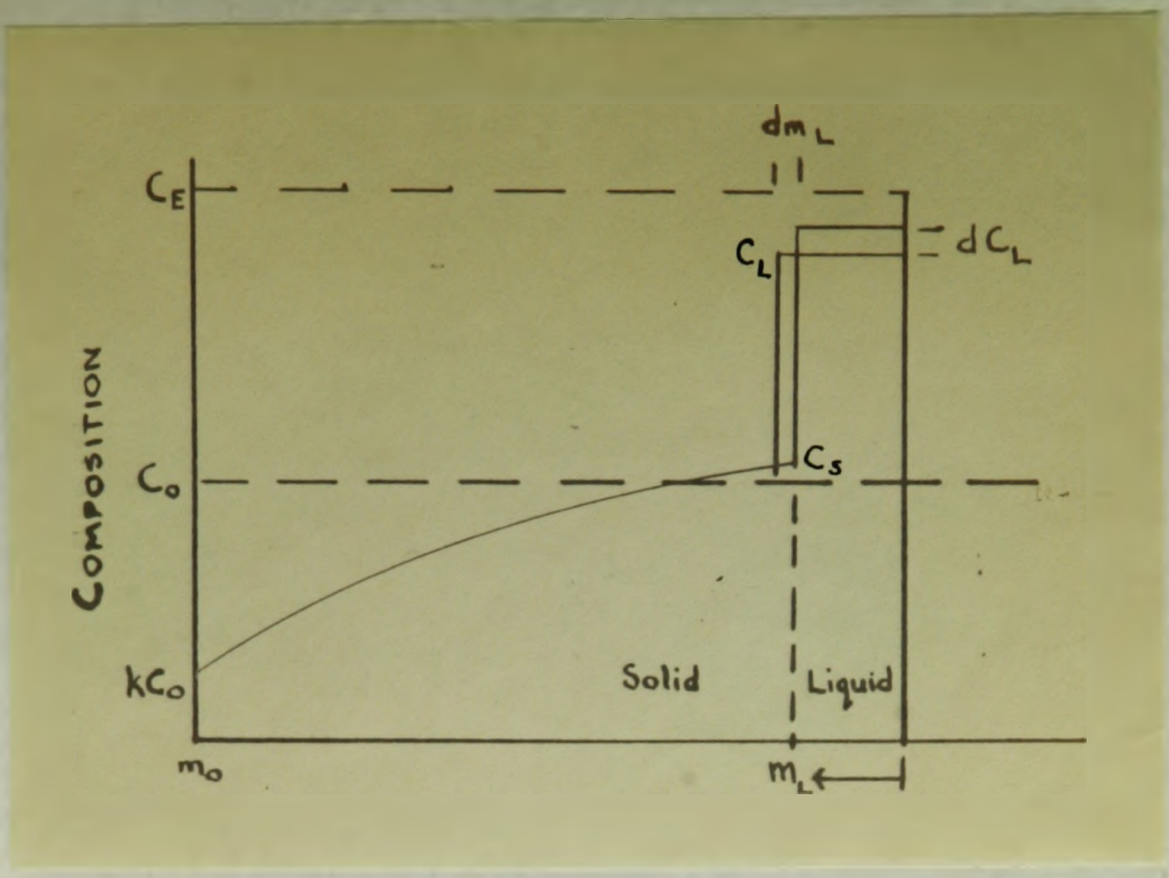

Fig. 6. Schematic non-equilibrium solute distribution.

On integrating from the initial liquid mass m_o to a final eutectic mass m_E and from C_o to C_E we obtain for the ratio of eutectic mass to initial mass

$$X_E = \frac{(m_E)}{(\overline{m_o})} = \frac{(C_E)}{(\overline{C_o})} = \frac{1}{1-K}$$

This means that even though there would be no eutectic for C_o smaller than kC_E resulting from equilibrium solidification, for actual non-equilibrium solidification, eutectic will persist in the microstructure even as $C_o \rightarrow 0$. We see mathematically that the segregation tendency of an element is monotonic with the segregation coefficient (1 - k), where k is the proportion of the element in the solid divided by the concentration of the element in the liquid according to the equilibrium diagram. This segregation condition is highly persistent for slowly diffusing substitutional elements in iron.

while soaking and working tend to moderate the segregation, coarse distributions arising in large slow-cooled ingots can persist with significant intensity into the final fabricated shapes. Fast-diffusing carbon, on the other hand, will have ample time to establish a transient equilibrium distribution in the austenite range. Chipman[10] has summarized this tendency for the important alloying elements in steel as shown in Table I.

As has been noted by many investigators [7,11,12,13], the presence of substitutional solutes in austenite has a profound effect on the activity of carbon. Carbon, since it can diffuse much faster than the segregated substitutional elements, will attain a non-uniform concentration in such a way as to equalize its thermodynamic activity in the alloy segregated surroundings. This type of carbon segregation can only be eliminated by bringing about a homogenization of the alloying elements. Presegregation as we call it, can produce only a small direct contribution to the final pearlite banding. However, it may significantly abet the more intense transformation segregation which has been described by Bastien[7].

When a hypoeutectoid steel transforms from the austenitic to the pearlitic structure it does so by rejecting ferrite when its temperature reaches the A_3 line, enriching the remaining austenite in carbon. Alloying elements such as manganese and silicon will lower or raise the A_3 point, and by doing so will cause the transformation to start at a higher or lower temperature. It can be seen that a steel segregated with such alloying elements will have different transformation temperatures in different areas. If we now consider a steel segregated in an alloying element such as

TABLE I

Solid-liquid distribution of source elements in iron (after Chipman[10]) +

Element	Atomic Weight	k, delta iron	Segregation Coefficient, 1 - k	
			Delta Iron	Gamma Iron
Aluminum	26.97	0.92	0.08	
Boron	10.8	(0.05)	(0.95)	(o.96)
Carbon[a]	12.0	0.13	0.87	0.64
Chromium	52.0	0.95	0.05	(0.15)
Cobalt	58.9	0.90	0.10	0.05
Copper	63.6	0.56	0.44	(0.12)
Hydrogen	1.0	0.32	0.68	0.55
Manganese*	54.9	0.84	0.16	0.05
Molybdenum	96.0	0.80	0.20	(0.4)
Nickel	58.7	0.80	0.20	0.05
Nitrogen	14.0	0.28	0.72	0.46
Oxygen[b]	16.0	(0.02)	(0.98)	(0.98)
Phosphorus	31.0	0.13	0.87	0.94
Silicon	28	0.66	0.34	(0.5)
Sulfur	32	(0.02)	(0.98)	(0.98)
Titanium	47.9	0.14	0.86	(0.93)
Tungsten	184.0	0.95	0.05	(0.5)
Vanadium	50.9	0.90	0.10	

+ The table given is an expansion from the original table published by Chipman.

* From the available phase diagrams it appears that the entries for delta iron for k and 1 - k are reversed.

silicon, which raises the A_3 line and presegregates the carbon away from the high silicon areas we will encounter the following effects. The high silicon areas being low in carbon and having a higher A_3 line will transform first, enriching the areas already high in carbon, until they ultimately attain the eutectoid (pearlite) composition. This effect occurs in reverse with such elements as manganese and chromium, which lower the A_3 line and presegregate carbon towards the high alloy regions. In both cases presegregation abets transformation segregation. On the other hand, one could imagine presegregation opposing transformation segregation if the A_3 line is lowered while presegregation of carbon occurs towards the highly alloyed areas of the steel, and vice versa. Such does not occur in the systems studied here but it may occur in the iron-carbon-nickel system.

In the above discussion and in our subsequent experimental work on presegregation we are concerned with the diffusion of carbon in a two-component matrix. This suggests that multicomponent ternary diffusion theory can be a useful tool for the analysis of the phenomenon. On the other hand, if we regard the presegregated state as one of transient equilibrium for carbon we can base an arithmetic description on the assumption of equalization of carbon activities.

THEORETICAL MODELS FOR PRESEGREGATION.

1) The Multicomponent Diffusion Model.

In an isothermal isobaric binary system of one phase where diffusion occurs in one direction only, Fick's first law [14] states that the quantity of diffusing substance which passes per unit time through unit area of a plane at right angles to the direction of diffusion, the flux J, is proportional

to the concentration gradient of the diffusing substance, viz.,

$$J = -D \frac{\partial C}{\partial X} \qquad (1)$$

where D is the diffusivity and $\partial C/\partial X$ is the concentration gradient. According to our previous thermodynamic considerations we know that a third element will have a profound influence on the distribution and therefore the diffusivity of carbon in iron. In order to describe this phenomenon we add a second term to Fick's equation[15] which accounts for the influence of the gradient of the third element on the flux of carbon, viz.,

$$J_1 = -D_{11} \frac{\partial C_1}{\partial X} - D_{12} \frac{\partial C_2}{\partial X} \qquad (2)$$

where

C_1 is the concentration of carbon in weight %;

C_2 is the concentration of the third element in weight %;

D_{11} is the ordinary diffusivity for carbon in iron. For dilute solutions this can be assumed independent of concentration.

D_{12} is the diffusivity of carbon for flow on the gradient of a third element. For dilute solutions the concentration dependance of D_{12} is given by $\frac{D_{12}}{D_{11}} = \alpha \bar{C}_1$ where α is a constant and $\bar{C}_1$ is the mean carbon concentration in the system.

Consider a closed, finite ternary system in which one of the diffusing components is extremely sluggish, so that its distribution is quasi-static, while the other independent component (let us say carbon in austenite) diffuses very rapidly. Fig. 7 shows a schematic concentration distribution in such a system at time zero and after a time for which the diffusion length for the carbon is appreciably greater than the dimension of the system, L. The state of the system will be called one of "transient equilibrium" if and when the carbon also attains a quasi-static distribution[17].

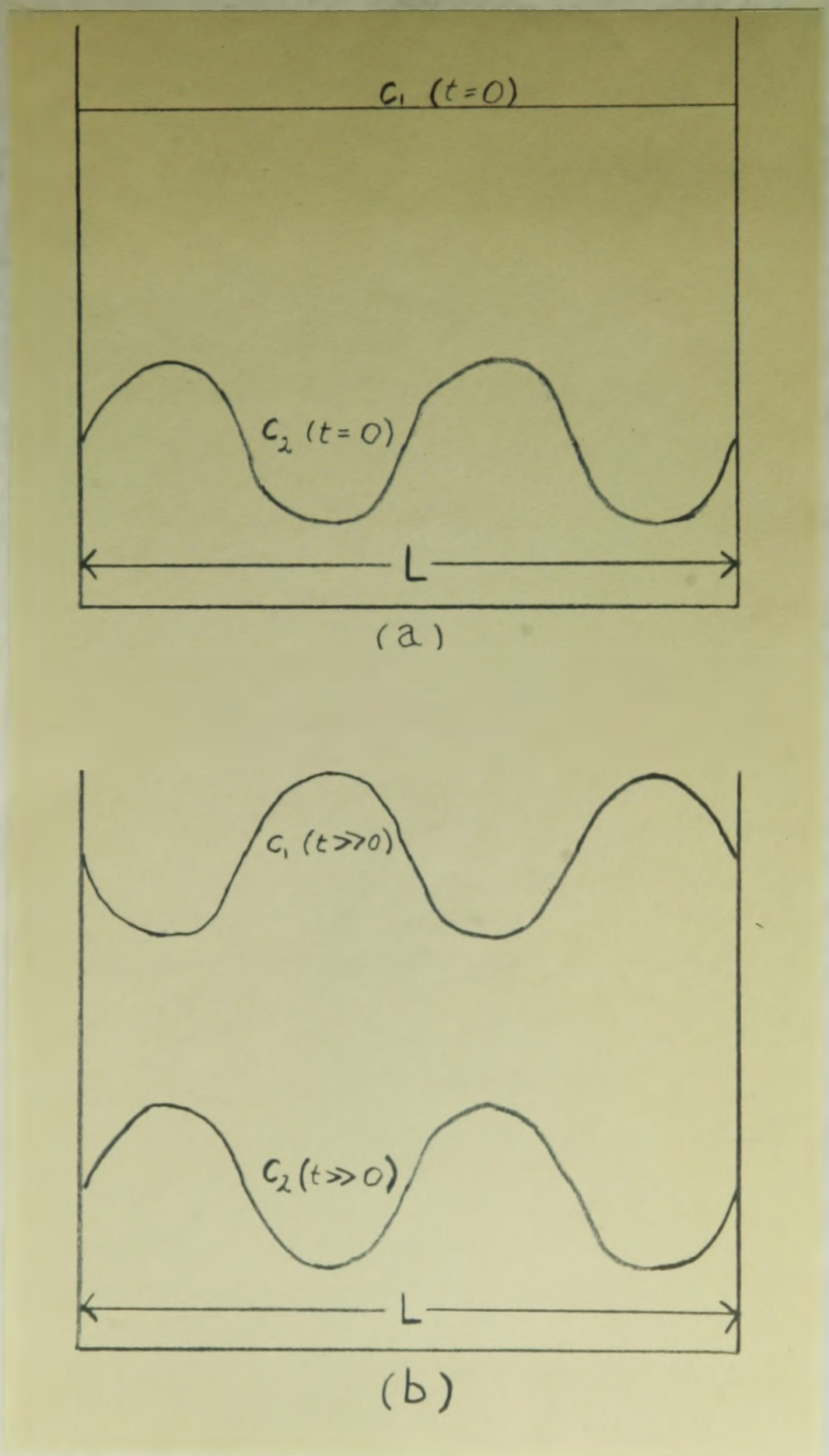

Fig. 7. Schematic representation of carbon and alloy concentration in a closed, finite system, a) at time t = zero; and, b) at time t greater than zero.

In terms of the diffusion flux, J_1, this state is necessarily described by $J_1 \sim 0$.

Consequently we can write equation (2) for the transient equilibrium state as

$$J_1 = -D_{11} \frac{\partial C_1}{\partial X} - D_{12} \frac{\partial C_2}{\partial X} = 0. \qquad (3)$$

This can now be integrated from the boundary to any intermediate point assuming the D's to be average values to give

$$C_1 = -C_2 \frac{D_{12}}{D_{11}} + A . \qquad (4)$$

Henceforth we will be considering the schematic system of Fig.8 for which the integral is carried from the surface to the center line. Such a solution can be used to analyze for diffusion data or, having such data available, to calculate concentration distributions in ternary systems such as might occur in the presegregation state of a banded steel. Some of the results of this investigation have been analyzed and compared with the multicomponent diffusion data of Darken[11] and Kirkaldy[18].

2) The Thermodynamic Model

The thermodynamic model for the presegregated state employs the assumption of uniform carbon activity at transient equilibrium. Up to approximately 1% carbon (by weight) and over the temperature range of 900°C - 1100°C the activity of carbon in austenite, a_c^γ, can be represented empirically by the equation

$$a_c^\gamma = N_c (1 + 7.25 N_c) \qquad (5)$$

where N_c is the mole fraction of carbon. The standard state is chosen so that Raoult's law is satisfied at infinite dilution.

Similarly, the activity of carbon in austenite in the presence of alloying element L can be represented approximately by the equation

$$a_{cL}^\gamma = N_c (1 + 7.25 N_c) (1 + dN_L) \qquad (6)$$

where d is a function of temperature. d has been established for silicon and manganese by Smith and Darken[20] at 1,000°C as +11.5 and -4.0, respectively. Evidently, silicon increases the activity of carbon in austenite while manganese decreases it.

We now consider an experimental three-layer diffusion couple which has attained transient equilibrium as represented by the schematic concentration distribution of Fig. 8

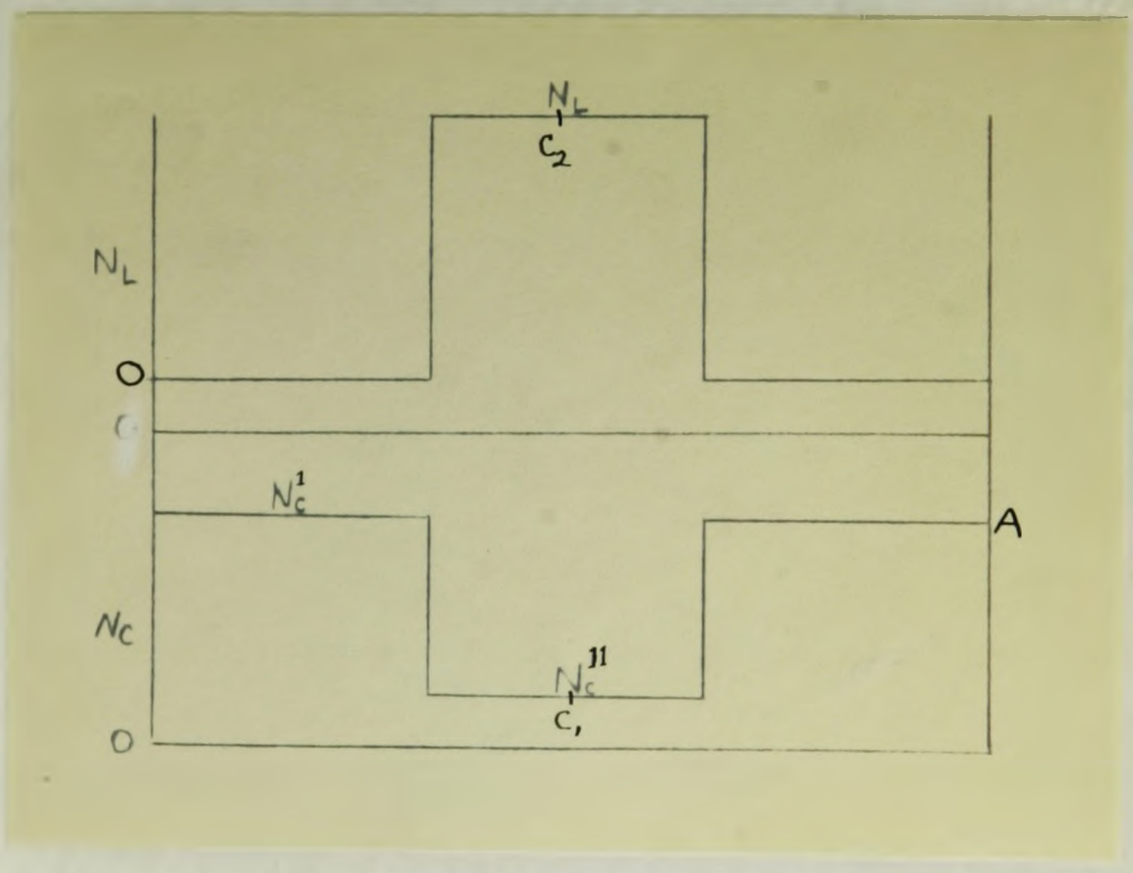

Fig. 8. Schematic representation of carbon and alloy distribution in an experimental three-layer couple at transient equilibrium.

(See experimental details of diffusion couple in following chapter). Since equal activities are assumed in the outside and inside layer at transient equilibrium, the equation to represent this situation can be written as:

$$N_c^1 \ (1 + 7.25\ N_c^1) = N_c^{11} \ (1 + 7.25\ N_c^{11}) \ (1 + d\ N_L) \quad (7)$$

The experimental concentration values obtained in the presegregation studies will be checked against equation (7) using the data of Smith and Darken.

II

EXPERIMENTAL

1) Preparation of Materials.

Most of the materials used were prepared in an induction melting unit under an argon atmosphere which was maintained above the melt by means of a transite hood as shown in Fig. 9. Melting time was of the order of 10 minutes and since the argon hood was sealed off, negligible oxidation occurred. Alloy additions were made via a copper pipe protruding through a hole in the top of the hood. Rapid and complete mixing of the additions was ensured through the natural swirling action of the induction heated melt. The mold was designed with a separate bottom to ensure easy removal of the ingot. The melt was cast in the form of a $1\frac{1}{2}$ inch diameter bar. For melting stock electrolytically refined iron was used. The cast material was then homogenized for one week at 1000°C in an argon atmosphere and furnace cooled. The silicon steel is a commercial electrical steel and was used as received. The iron-carbon alloy which was used for the outside layers of all the diffusion couples, was supplied by Ford Motor Research Laboratories, Detroit. Table II gives the compositions of the alloys used:

TABLE II. Table of alloy compositions.

MATERIAL	%C	%Cr	%Mn	%P	%Si
4% Cr - Fe	.009	4.00	.04	.003	.030
3.3% Mn-Fe	.202	.034	3.30	.015	.027
0.5% P-Fe	.262	.017	.03	.525	.001
0.9% P-Fe	.153	.024	.02	.900	.030
1.5% Si-Fe	.070	.010	.18	.088	1.50
0.4% C-Fe	.406	.002	.01	.006	.001

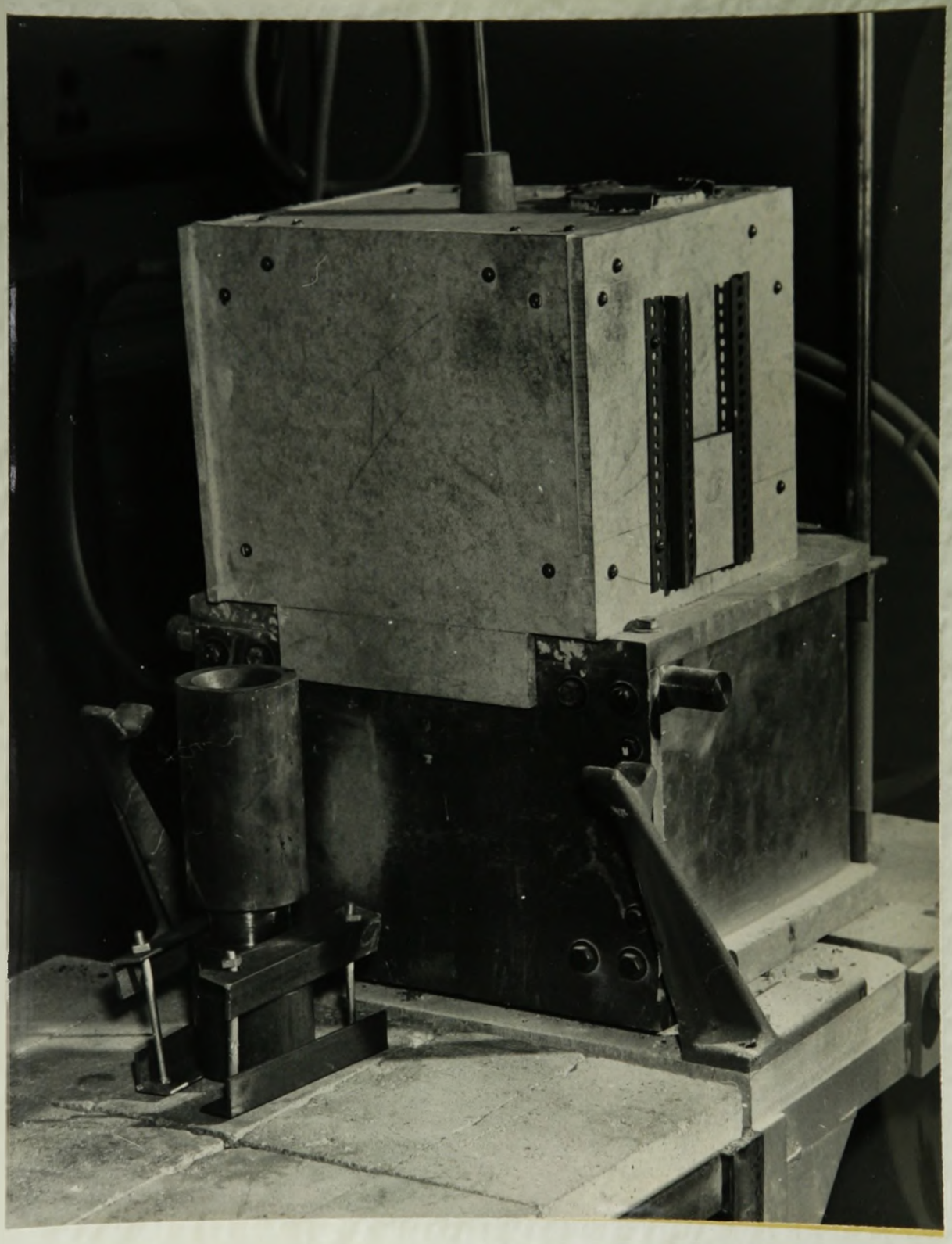

Fig. 9. Photograph of induction melting unit with transite hood and mold.

2) Design of Diffusion Couples to Simulate Banding.

The bars were turned to one inch round to get rid of any possible decarburization. No decarburization could then be detected metallographically. The bars were then cut on a cut-off wheel to platelets of approximately 0.050 inch thick. The design thickness for the iron-carbon platelets was 0.035 inches and for the iron alloy platelets 0.040 inches. The difference was due to the fact that in the next step, the grinding of the platelets on a surface grinder, both sides had to be ground on the alloy-iron platelets, while only one side of the iron-carbon platelets had to be ground. In this way all platelets were ground to 0.030 $\pm$ 0.001 inches. The platelets were then arranged with the iron alloy in the centre of a couple and with an iron carbon platelet on each side. This arrangement was found most satisfactory, since it minimizes the time for the couple to come to transient equilibrium. The couples were then separated by a thin sheet of mica to prevent diffusion between them. They were then damped firmly together in a holder as shown in the schematic diagram of Fig. 10.

Two 18 - 8 stainless steel spacers were inserted into the plain carbon steel clamp to ensure increasing pressure as the temperature rises due to the larger expansion coefficient of stainless steel. The clamp and couples were then welded into an inconel retort which was equipped with two access tubes to conduct the desired atmosphere. The couples were heated to temperature and first held there for 10 to 12 hours in a hydrogen atmosphere. The hydrogen was used to reduce the oxide on the contact surfaces to aid welding. The hydrogen was purified by passing it through a commercial "DEOXO" purifier. This method of welding proved very successful

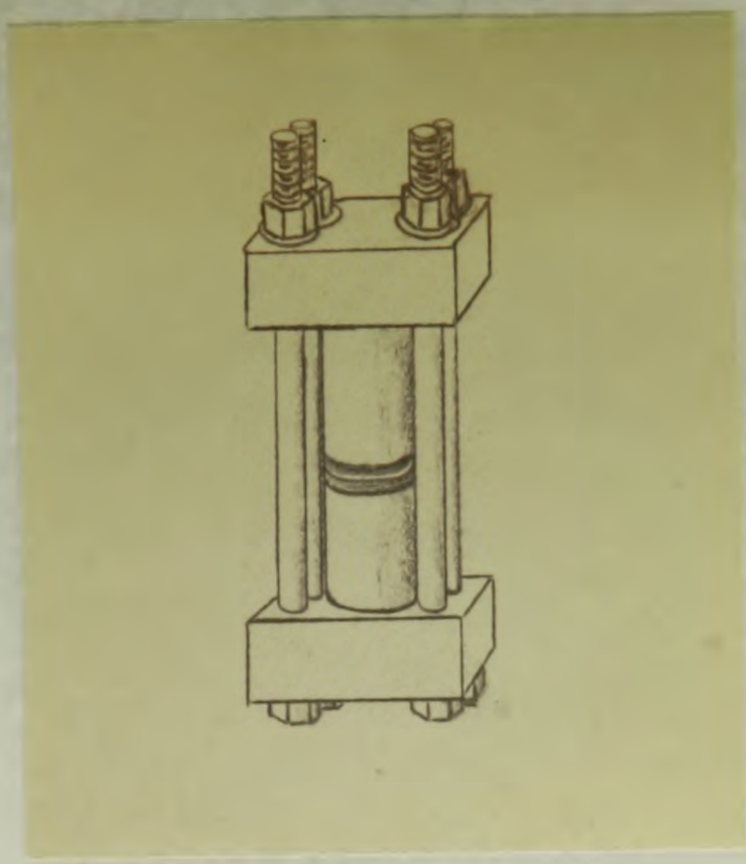

Fig. 10. Schematic diagram of couple clamp showing two layerdiffusion couples in place.

as can be seen from the photomicrographs of a later section. A drawback to the hydrogen welding method is that there occurs a decarburization of the couples due to the reaction

$$2\,H_2 + C \leftrightharpoons CH_4. \qquad (8)$$

This reaction will proceed for the full length of time that the couples are in the hydrogen atmosphere since the reaction product is swept out of the retort due to the continuous flow of hydrogen. The decarburization has no effect on the experimental interpretations since it only lowers the total amount of carbon present.

The couples were finally allowed to diffuse in an argon atmosphere

for suitable times over a range of interesting temperatures. The couples were then quenched in an accelerated argon flow at the rate of approximately 50°C per minute to prevent transformation segregation. A photograph of the furnace, retort and clamp is shown in Fig. 11.

The necessary diffusion times for attainment of transient equilibrium at various temperatures were estimated according to the requirement that the diffusion length, $\sqrt{Dt}$, be at least seven times the half-thickness of the couple. That the carbon distribution does come to transient equilibrium was checked in a preliminary experiment with silicon alloy couples in which platelets of three different thicknesses, 0.020, 0.035 and 0.050 inches were allowed to diffuse for a time calculated to be sufficient for the intermediate and smaller thicknesses. Even the heaviest couple attained very close to transient equilibrium, since no carbon gradient could be detected metallographically across the width of any one platelet. Fig. 12(a) is typical of the result obtained for all couples in this test. The actual test couple layer thickness was chosen at 0.030 inches so as to obtain at least two grams of sample from each platelet for analytical purposes.

3) Sectioning and Analyses.

The couples were sectioned for analyses by clamping them into a special one inch lathe collet and machining parallel to the surface down to a diameter of $\frac{1}{4}$ inch. 0.003 to 0.005 inches on each side of the weld were cut out to ensure that no foreign material was present in the sample and avoid any transformation effects in this region. The last $\frac{1}{4}$ inch diameter of sample was reserved for metallographic work. Great precaution was taken so as not to get any oil or carbonaceous material from the lathe onto the sample. The samples ranged between twoand three and one-half grams, so

Fig. 11. Photograph showing furnace arrangement with retort and clamp.

that two or three chemical analyses could be made on each sample. The analyses were made on a Leco Model # 600OH Carbon Determinator. The analytical results are given in Table III.

4) Segregation on Transformation.

An auxiliary set of couples was constructed as described in the previous section. These were again left to diffuse at 990°C until transient equilibrium was attained. The couples were then furnace cooled at the rate of 1.2°C per minute. They were then quartered and two of the sections were given a subsequent solution treatment at 990°C for two hours and cooled at rates of 4.0°C a minute and 7.5°C a minute, respectively.

These slow cooling rates allow the development of a form of segregation in the diffusion couples which is closely akin to the intense transformation segregation which occurs in banded steels. This segregation appears near the weld and is connected with the steep gradient of substitutional alloying element existing at this point. The micrographic results of these tests are given in Figs. 12 - 16 and the corresponding quantitative measurements of band widths are given in Table IV.

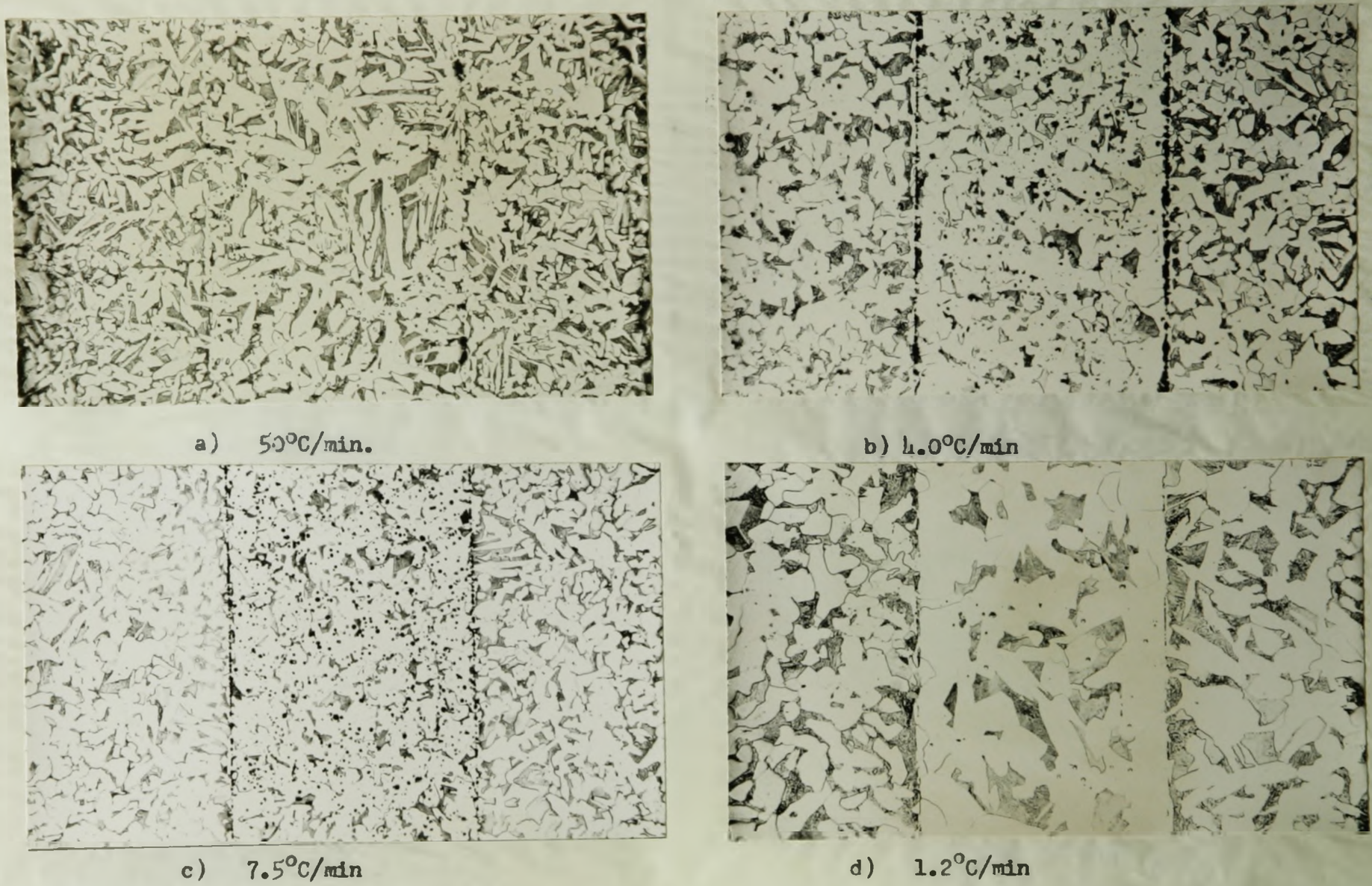

a) 50°C/min.

b) 4.0°C/min

c) 7.5°C/min

d) 1.2°C/min

Fig. 12. Micrographs of silicon alloy diffusion couples undergoing different cooling rates from the soaking temperature of 990°C. 535X

a) 50°C/min

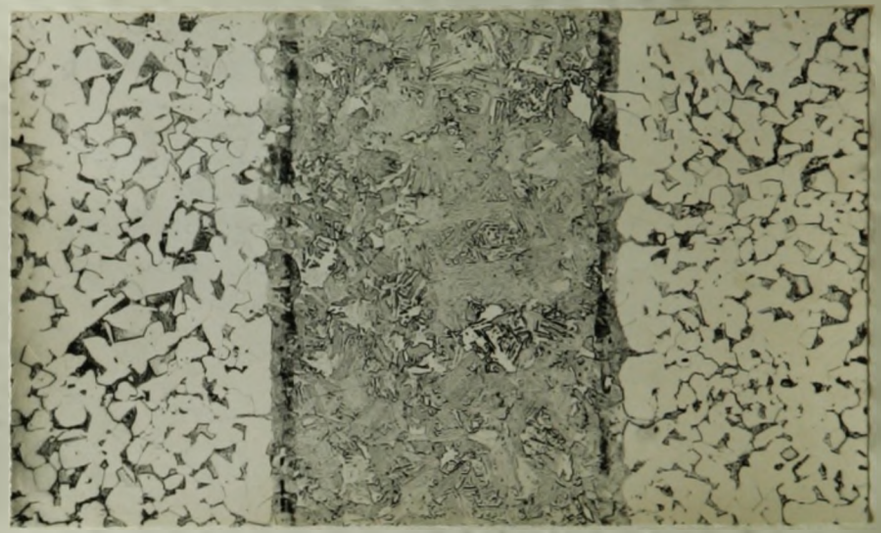

b) 4.0°C/min

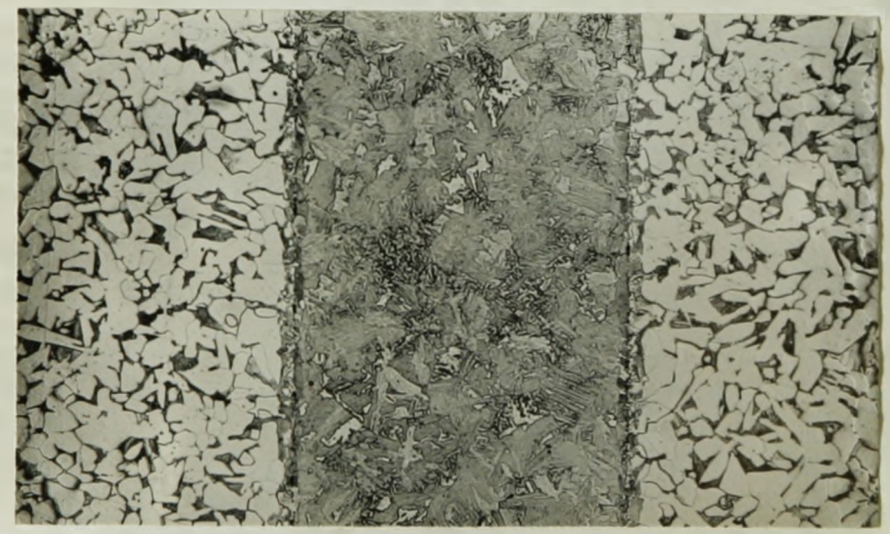

c) 7.5°C/min

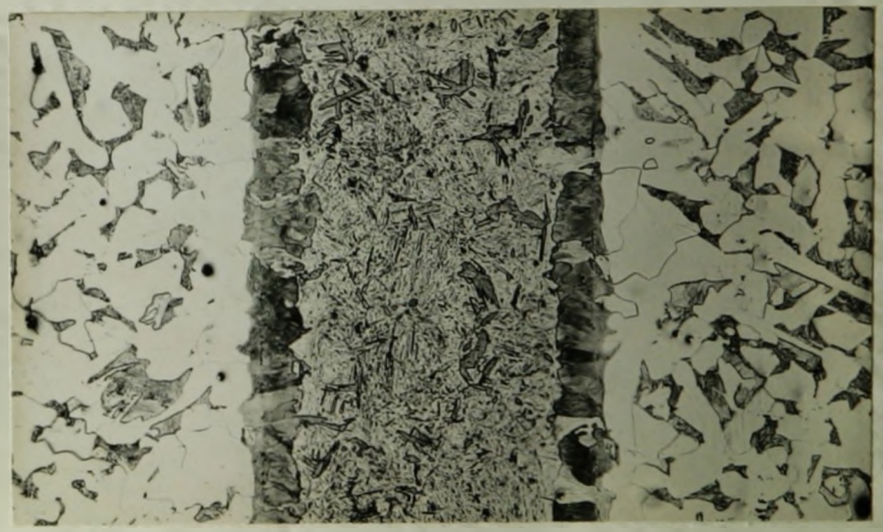

d) 1.2°C/min

Fig. 13. Micrographs of manganese alloy diffusion couples undergoing different cooling rates from the soaking temperature of 990°C. 535 X

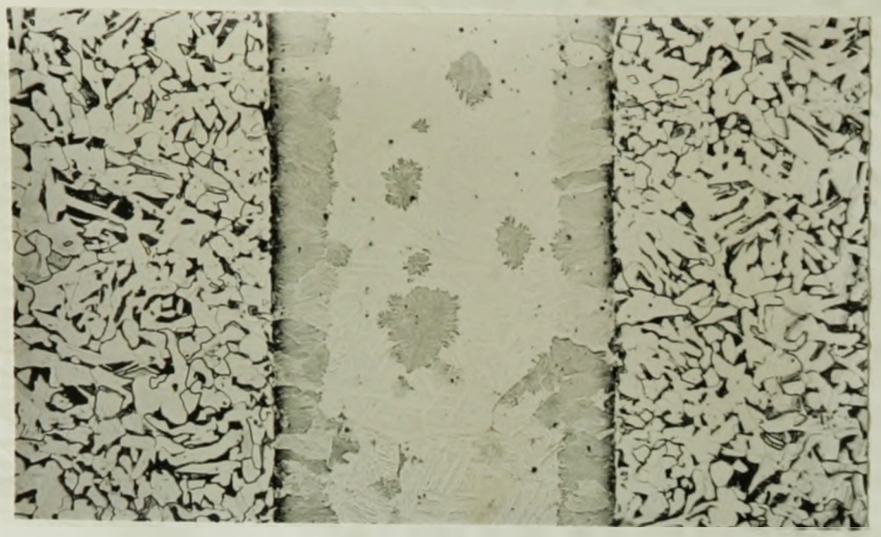

a) 50°C/min

b) 4.0°C/min

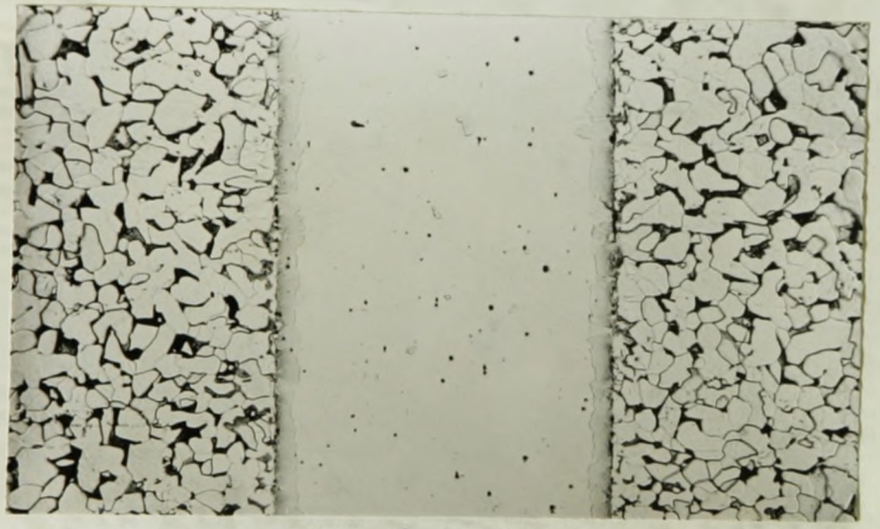

c) 7.5°C/min

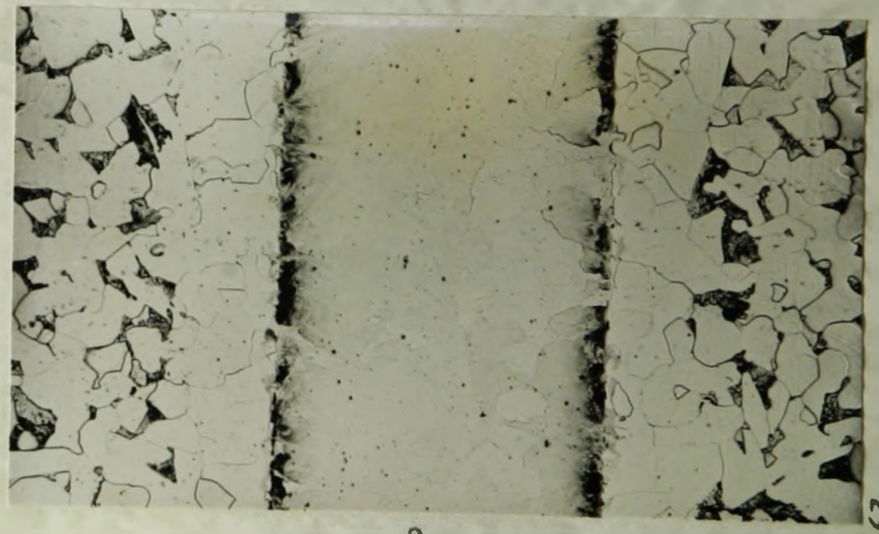

d) 1.2°C/min

Fig. 14. Micrographs of Chromium alloy diffusion couples undergoing different cooling rates from the soaking temperature of 990°C. 53 5X

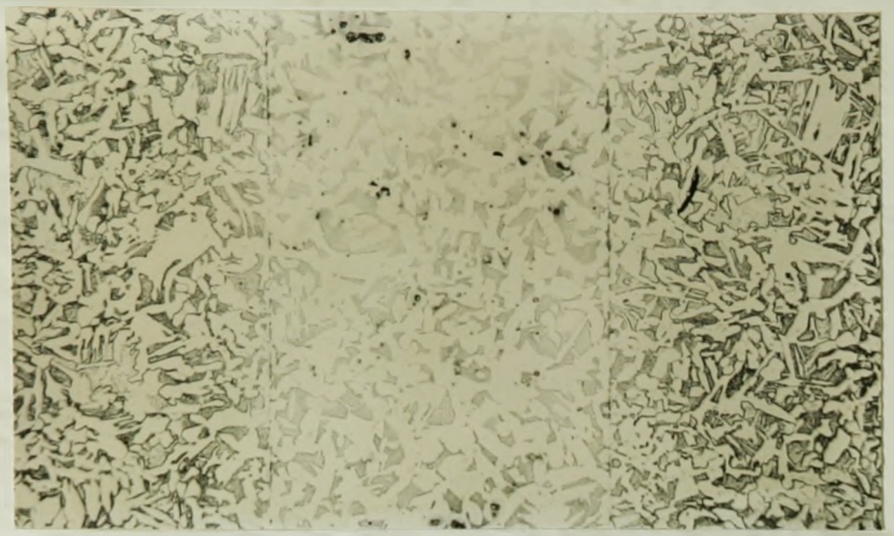

a) 50°C/min

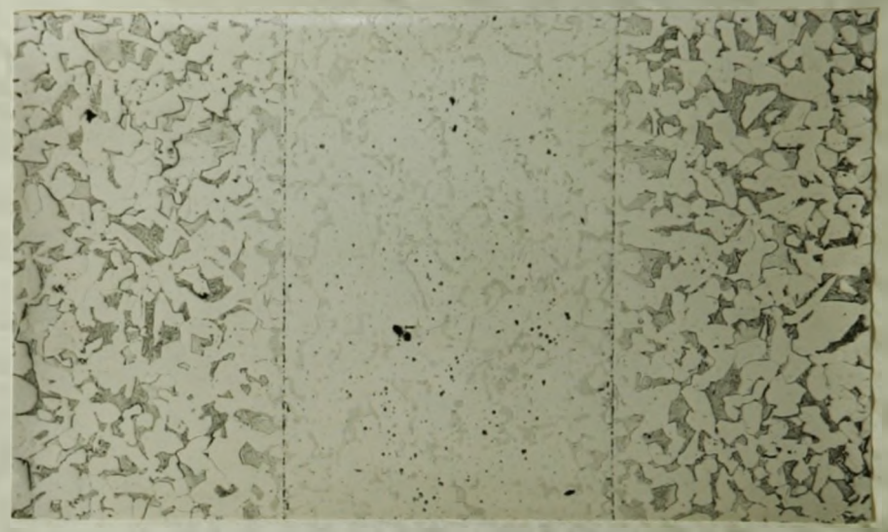

b) 4.0°C/min

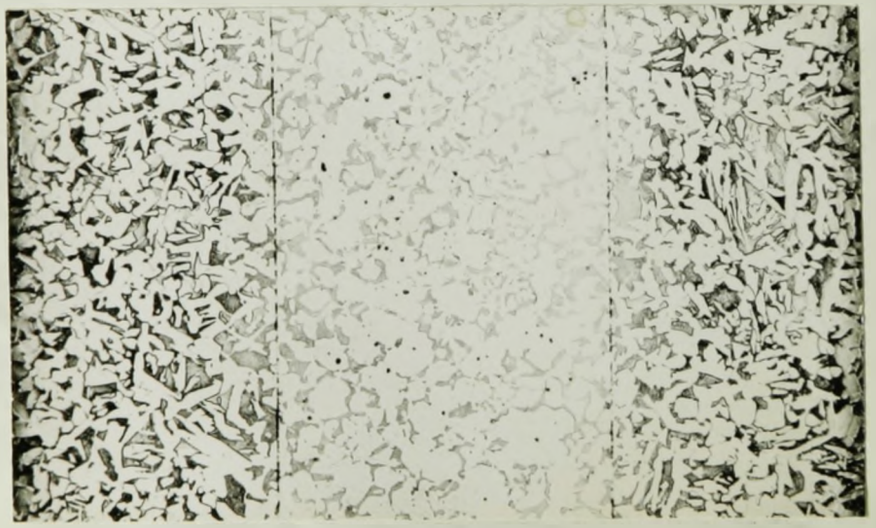

c) 7.5°C/min

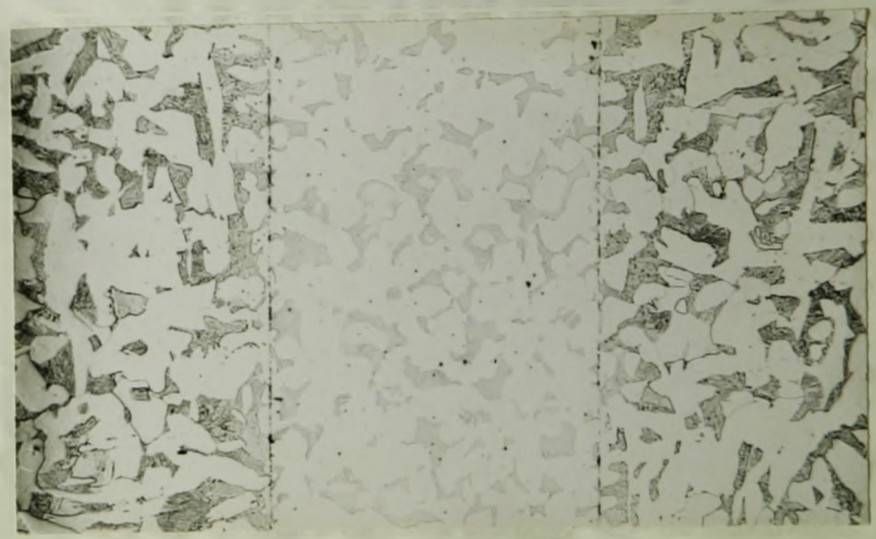

d) 1.2°C/min

Fig. 15. Micrographs of 0.525% Phosphorus alloy diffusion couples undergoing different cooling rates from the soaking temperature of 990°C. 535 X

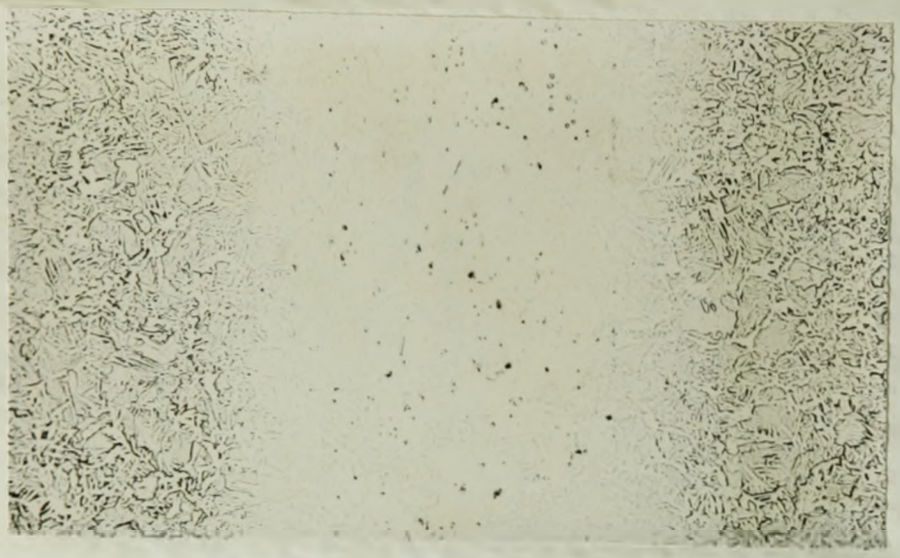

a) 50°C/min

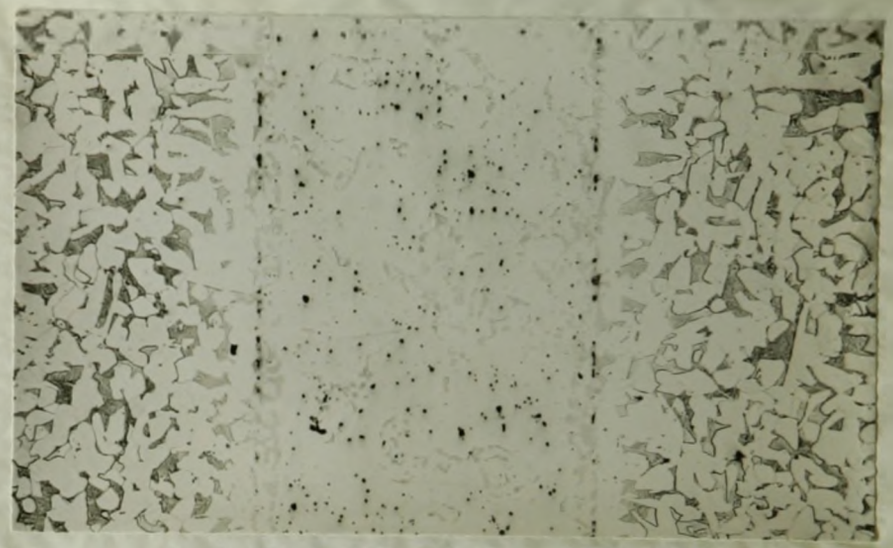

b) 4.0°C/Min

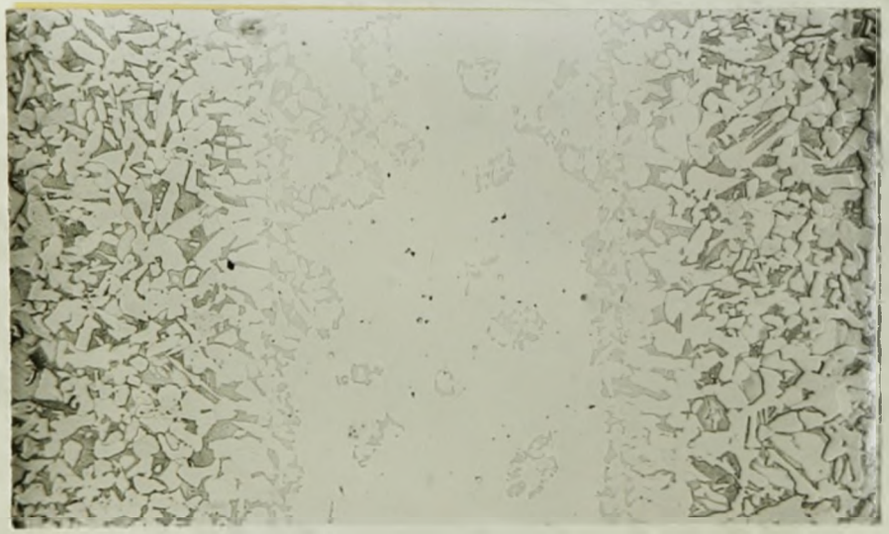

c) 7.5°C/min

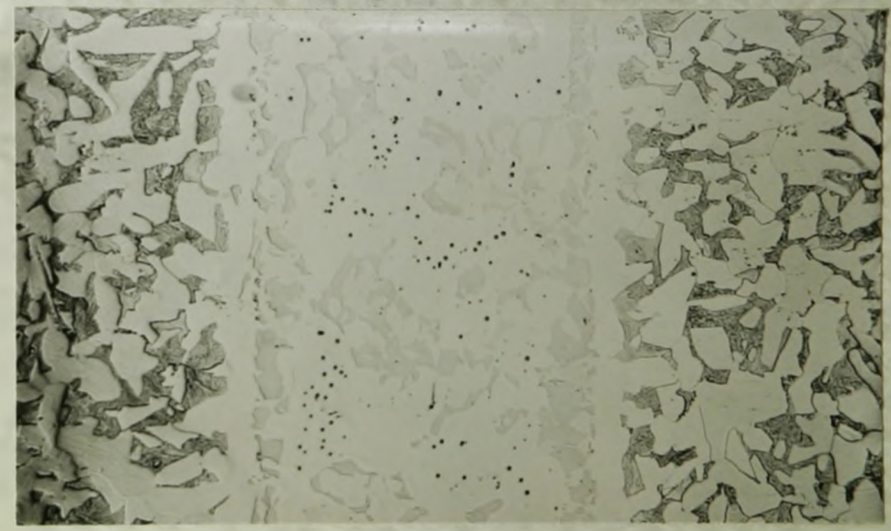

d) 1.2°C/min

Fig. 16. Micrographs of 0.9% Phosphorus alloy diffusion couples undergoing different cooling rates from the soaking temperature of 990°C. 535 X

III

RESULTS

TABLE III. Table giving final analyses of presegregated three-layer couples.

Couple	Temp. (°C)	% Carbon A	C_1	A	Mean % Carbon $(A+C_1)/2$	Difference % C, $(A-C_1)$	Presegregation coeff. $\alpha = (A-C_1)/(C_2-C_1)$
Fe-1.5% Si-Fe	1050	.256	.223	.256	.239	+.033±.013*	.092 ± .036
	990	.277	.218	.277	.248	+.059±.007	.160 ± .019
	950	.250	.206	.250	.228	+.044±.010	.128 ± .029
	930	.314	.259	.314	.286	+.055±.010	.130 ± .023
Fe-.525% P-Fe	1050	.297	.252	.297	.274	+.045±.010	.32 ± .070
	990	.294	.250	.294	.274	+.049±.010	.34 ± .070
	950	.316	.210	.316	.263	+.106±.011	.79 ± .080
	930	.383	.276	.383	.329	+.107±.011	.62 ± .060
Fe-3.3% Mn-Fe	1050	.261	.286	.261	.273	-.025±.010	.028 ± .011
	990	.273	.323	.273	.298	-.050±.010	.051 ± .010
	950	.265	.330	.265	.298	-.065±.007	.066 ± .007
	930	.314	.361	.314	.337	-.053±.011	.048 ± .010
Fe-4% Cr-Fe	1100	.225	.311	.225	.268	-.086±.012	.080 ± .011
	1050	.199	.282	.199	.240	-.083±.013	.087 ± .013
	990	.206	.340	.206	.273	-.134±.010	.123 ± .009
	950	.187	.292	.187	.239	-.105±.010	.111 ± .010
	930	.236	.357	.236	.296	-.121±.011	.102 ± .009

* Errors are r.m.s. values determined from the measured deviations of the carbon analyses.

TABLE IV. Table showing experimentally measured band widths at different cooling rates.

Couples	Rate of Cooling $\dot{T}$(°C/min)	D ave. x10^{+8}	ΔT estim. (°C)	$W \sim \sqrt{\frac{D\Delta T}{\dot{T}}}$ estim.(cm)	Band width (cm) measured
Fe-1.5% Si-Fe	1.2	7.4	120	.021	.0122
	4.0			.012	.0080
	7.5			.0084	.0050
	50.0			.0032	0.0
Fe-.525% P-Fe	1.2	Insufficient			0.0
	4.0	data			0.0
	7.5				0.0
	50.0				0.0
Fe-.9% P-Fe	1.2	Insufficient			.0104
	4.0	data			.0055
	7.5				.0034
	50.0				0.0
Fe-3.3% Mn-Fe	1.2	1.5	100	.009	.012
	4.0			.0045	.0088
	7.5			.0035	.0039
	50.0			.0013	0.0
Fe-4.0% Cr-Fe	1.2	4.0	60	.007	.019
	4.0			.006	.012
	7.5			.0044	.0055
	50.0			.0017	0.0

DISCUSSION OF RESULTS

1) Discussion of Presegregation Results.

Table III summarizes the data to be discussed in this section. As can be seen from figs. 12(a) to 15(a) transient equilibrium was obtained in

all couples. Furthermore, the method of quenching with an argon blast (cooling rate 50°/min) resulted in a complete elimination of transformation segregation. The magnitude and sign of the presegregation as measured by the carbon concentration difference between adjacent layers, agrees with the thermodynamic predictions for the silicon and manganese containing couples. In general, the sign of the segregation is in agreement with the rule of Jatszak et al[5] that carbide formers (manganese and chromium) attract carbon while solution elements (silicon and phosphorus) reject it. There is a bias for decrease in amount of presegregation with increasing temperature.

To compare the silicon and manganese results with the thermodynamic predictions we have substituted the experimental values for N_L and N_c^{11} into equation (7) and calculated N_c^1. We have then recorded in Tables V and VI the difference A (theor) - C_1 (exp) for comparison with the experimental difference. The sign of the prediction is confirmed in both cases while the magnitude shows fair agreement with experiment. The deviations are not unexpected since no temperature dependence has been recorded in the literature for the thermodynamic coefficients, d.

To check the temperature dependence of the pre-segregation we must invoke the multicomponent diffusion formalism to remove the concentration dependence in our data. Referring to equation (4) and applying it to our couple configuration we can let C_1 and C_2 represent the inner layer concentrations. Thus, to satisfy the boundary conditions, A must equal the outer carbon concentration. The ratio D_{12}/D_{11} is then given by

$$\frac{D_{12}}{D_{11}} = \frac{A - C_1}{C_2} \qquad (8)$$

[6]

However, for theoretical reasons we have

$$\frac{D_{12}}{D_{11}} = \alpha \bar{C}_1 \qquad (9)$$

where α will be a function of temperature only.

TABLE V. Table comparing calculated and experimental values of the presegregation for the silicon couples.

T (°C)	Inner Layer experimental		Outer Layer theoretical		Presegregation (wt %) A - C_1	
	C_1	N_c^{II}	A	N_c^{I}	theor.	exper.
1050	.223	.0104	.257	.0172	.034	.033 ± .013
990	.218	.0101	.247	.0165	.029	.059 ± .007
950	.206	.0096	.230	.0154	.024	.044 ± .010
930	.259	.0121	.282	.0189	.023	.055 ± .010

TABLE VI. Table comparing calculated values of $(N_c^{II} - N_c^{I})$ and experimental values for the manganese couples.

T (°C)	Inner Layer experimental		Outer Layer theoretical		Presegregation (wt %) A - C_1	
	C_1	N_c^{II}	A	N_c^{I}	theor.	exper.
1050	.286	.0133	.245	.0114	-.041	-.025 ± .010
990	.323	.0150	.262	.0122	-.061	-.050 ± .010
950	.330	.0153	.260	.0121	-.070	-.065 ± .007
930	.361	.0168	.310	.0144	-.051	-.053 ± .011

Solving, we obtain

$$\alpha = \frac{A - C_1}{C_2 \cdot C_1} \qquad (10)$$

and this is the quantity which we must investigate for temperature dependence. The last column of Table III shows this quantity as a function of temperature and it is plotted for the four couples in Fig. 17. In every case there appears to be a sharp drop in α with increasing temperature. This may be

simply a manifestation of the tendency of solutions to approach closer to ideality with increasing temperature.

Multicomponent diffusion data is available only in the system iron-silicon-carbon. Kirkaldy[18] in an analysis of Darkens diffusion data[11] has given $\alpha = D_{12}/D_{11}\,\bar{C}_1 = 0.154$ at 1050°C. The present data gives via relation 10, $\alpha = 0.110$ (See Fig. 17). The comparison is sufficiently good as to recommend the transient equilibrium couple technique as an efficient method for determining multicomponent diffusion data.

2) Discussion of Transformation Segregation.

The thermodynamic carbon presegregation discussed above is a relatively weak effect compared to the intense carbon segregation which appears in the room temperature microstructure of commercial steels (see Fig. 1). This intense segregation must accordingly occur during the transformation on cooling.

With the data accumulated here and elsewhere we now have the means to produce a semiquantitative theory of banding. To summarize: we have established the sign and magnitude of the carbon presegregation occurring in various ternary systems and noted that the magnitude of this tendency invariably increases as the austenitic soaking temperature approaches the A_3 line (see Table III and Fig. 17). With Bastien[7] we have noted that the position of the A_3 line is a sensitive function of the alloy content and data from various sources[21] have allowed us to record this function for most of our systems as shown in Fig. 18. Finally, in cooling our diffusion couples at various rates we have been able to produce banding in the weld regions of an intensity equal to that obtained in commercial situations (see Figs. 13 to 16.) This simulated transformation segregation arises

from a slightly different boundary condition than the commercial effect but its fundamental cause is identical to that producing banding in commercial steels. We shall therefore first produce an explanation of our observations, and later extend this to the commercial configuration.

a) The silicon couples.

Consider for illustrative purposes the transformation characteristics for the Fe-Si-C couples described by the 990°C entry of Table III. The concentration and activity distributions of this couple in the transient equilibrium state are sketched in Figs. 19(a) and (b). Since silicon is a weak hardenability agent[21] we can discuss the transformation characteristics qualitatively by reference only to the equilibrium constitution diagrams of Fig. 19 rather than to the appropriate TTT curves of the various layers of the couple. The two transient equilibrium concentrations and their difference are indicated on that Figure. Now, as the couple is slowly cooled (at 1.2°C/min) towards the A_3 line the activity curve will be altered towards that of Fig. 19(d) due to the increase in the presegregation coefficient given by Fig. 17(b). There might be a slight corresponding redistribution of the concentration distribution as the inner silicon-rich layer attains the A_3 line, as indicated in Fig. 19(c). Shortly thereafter ferrite will nucleate at the point marked F and other excess carbon will be swept along the continuously increasing carbon activity gradient into the outer layers. The beginning of transformation anywhere in this outer layer will be delayed at least for a time corresponding to the temperature drop ΔT. In the region adjacent to the weld, marked P, which is being continuously enriched by transport of carbon from F, the start of the ferrite transformation may be completely suppressed. This region, being finally enriched to the

eutectoid concentration, will become completely pearlitic. The final result is the banded structures of Figs. 12 and 19(e). It is possible to estimate the band width w for this configuration (indicated on Fig. 19(e)) by noting that it must be of the order of the diffusion length at the mean temperature of the interval ΔT and for a time corresponding to Δt. If the cooling rate in this interval is $\dot{T} = dT/dt = \Delta T/\Delta t$ then

$$w \sim \sqrt{D\ t} = \sqrt{D\ \Delta T/\dot{T}} \qquad (11)$$

It should be particularly noted that the magnitude of ΔT is determined in part by the amount of presegregation $A - C_1$ and by the shift of the A_3 line in alloy-rich regions. Table IV gives a comparison of the estimated and measured band width for the silicon couple. There is good order of magnitude agreement for the slow cooling rates. No comparison is possible for the fast-cooled sample since it is not possible to detect a band when its width becomes appreciably less than the grain size.

b) The manganese and chromium couples.

The above considerations are completely reversed for the chromium and manganese couples since these elements depress the A_3 line and show a negative presegregation, $(A - C_1)$. Thus the pearlite band appears in the alloy-rich region. A detailed discussion of these systems is rather more complex than the silicon system since here the hardenability effects are very strong. This is evident from the microstructures of Figs. 13 and 14 where bainite or martensite appears in the chromium-rich layer and martensite appears in the manganese-rich layer. The net effect of the hardenability factor is to abet banding since transformation is further delayed in the alloy-rich regions. We have ignored this factor in estimating the band widths of Table IV.

c) The 0.525 phorphorus couples.

The 0.525 phosphorus couple produced a startling result since no banding appeared at any of the cooling rates (see Fig. 15). Since the effect of phosphorus on the A_3 line is supposed to be similar to silicon[7] and presegregation is very strong and of the same sign as silicon (Table III) we expect the banding to be similar. The null observation might be attributed to the large hardenability effect of phosphorus noted by Bastien[7]. With reference to the TTT curves of Fig. 4 it was surmised that in a certain range of cooling rates banding could be eliminated. We could have fortuitously chosen our cooling rates in such a critical range. On the other hand, the absence of banding may be a simple consequence of the fact that the effective T is too small for this rather dilute alloy to produce detectable bands. We are rather inclined to favour the latter explanation since the former does not appear to be quantitatively consistent. Furthermore, the results for the 0.9 phosphorus couples are understandable without the invocation of the hardenability factor.

d) The 0.9 phosphorus couples.

The metallographic results for these couples (Fig. 16) are complex since the phosphorus-rich (inside) regions appear to remain mostly ferritic at soaking temperatures. Thus the couple at transient equilibrium is two-phase. The ternary phase diagram for this system indicates that the austenitic (outside) regions will precipitate ferrite. This precipitation will first occur adjacent to the phase boundary and carbon will be swept outward on the activity gradient provided by the phosphorus distribution. Fig. 20(a) shows the schematic microstructure of the couple at soaking temperature, 20(b) shows it during transformation while 20(c) shows

the final micrographic result. We note that the relative segregation that occurs in precipitation of ferrite from the austenite has the same direction as in the silicon couples and is just as would be predicted when hardenability effects are ignored.

e) Technological significance of the results.

The results for the silicon, manganese and chromium couples were not unexpected. The direction of segregation is in agreement with the rules of Jatzak et al[5] that solution-type alloys (silicon and phosphorus) reject carbon while carbide formers (manganese and chromium) attract it. The unexpected behaviour of the phosphorus couples may force a revision of current ideas about "phos-banding" since it appears that such can occur with intensity only if there is sufficient phosphorus to maintain the ferritic state at soaking temperatures (~1½). "Phos-banding" has thus far been regarded as arising purely from transformation of austenite[5,7].

It is apparent from the cooling rate tests that banding can be minimized by fast cooling (usually normalizing rather than annealing). It is possible to use the qualitative theoretical considerations leading to relation (11) to estimate the minimal cooling rates. In a banded steel, the band width is fixed by the alloy segregation. To prevent transformation segregation it is necessary that the diffusion length corresponding to the temperature differential ΔT (see Fig.18) be appreciably less than the band width, i.e.,

$$\dot{T} > \frac{D \Delta T}{w^2} \qquad (12)$$

This estimate gives results which are in agreement with the commercial tests of Plockinger and Randak[6].

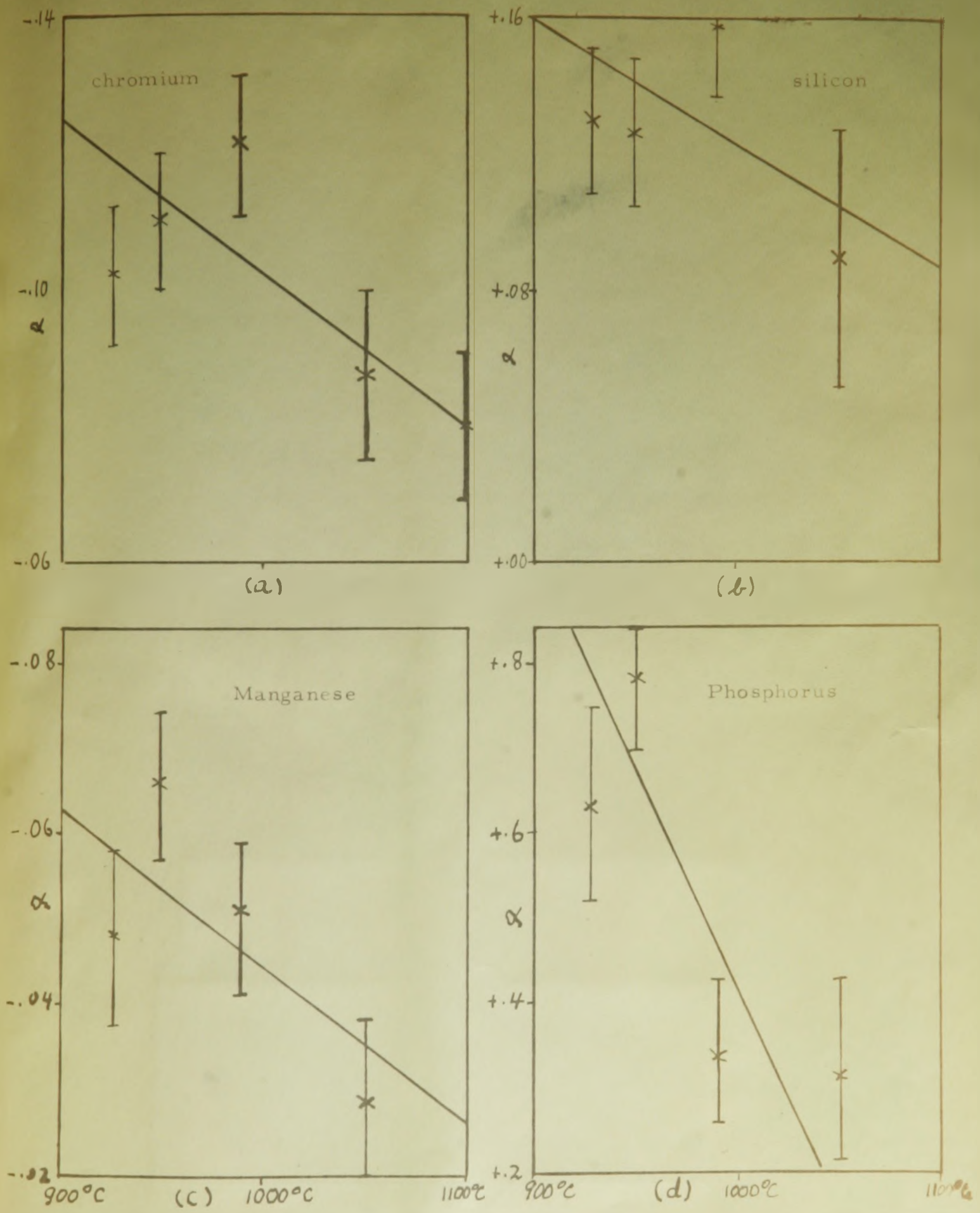

Fig. 17. Temperature dependence of the pre-segregation coefficient $\alpha = A\text{-}C_1/C_2\,C_1$ (see Table III) r.m.s. errors are determined from the scatter in the experimental carbon determinations.

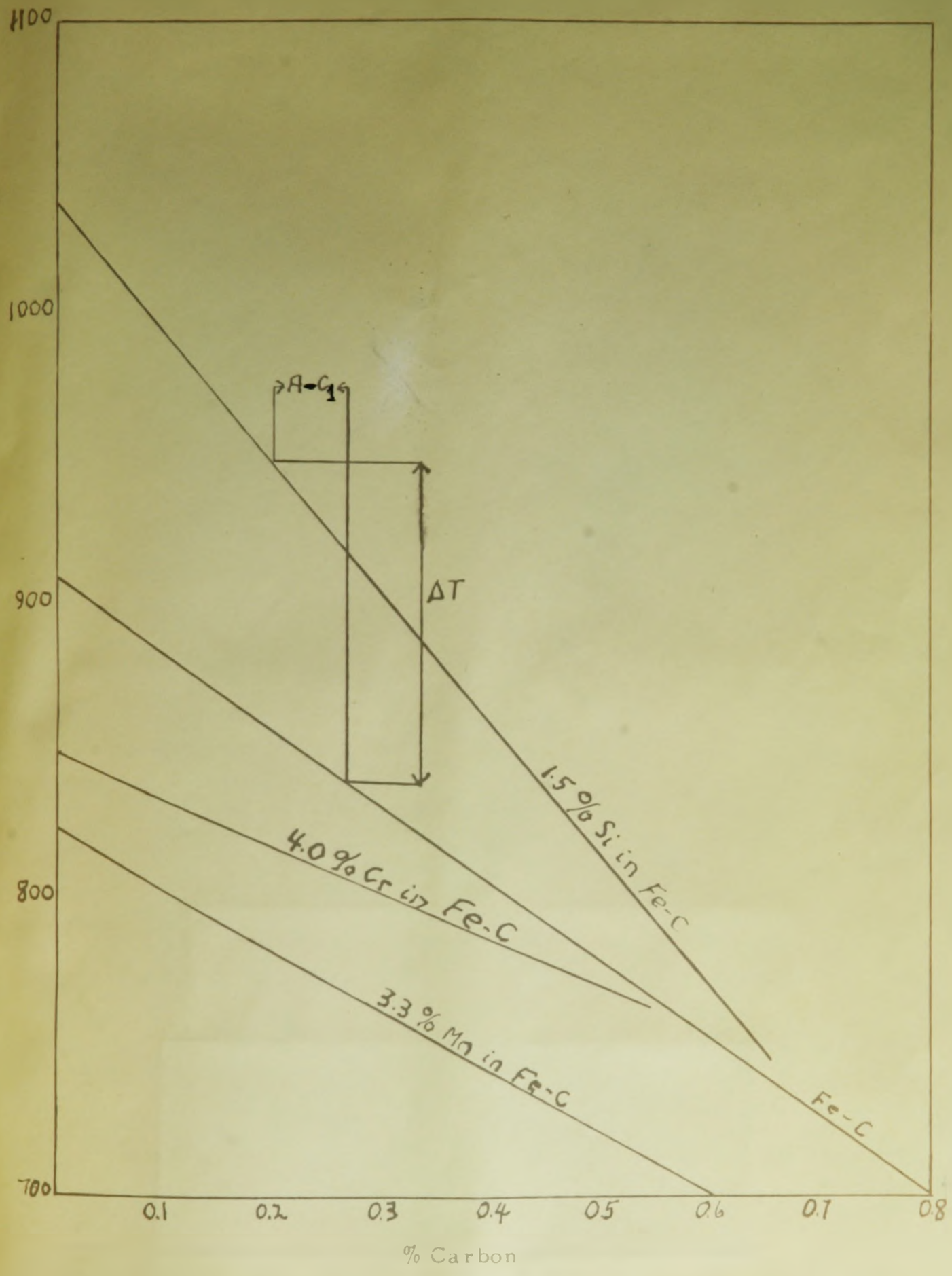

Fig. 18. Variation of the A_3 line with specific amounts of different alloying elements[21]

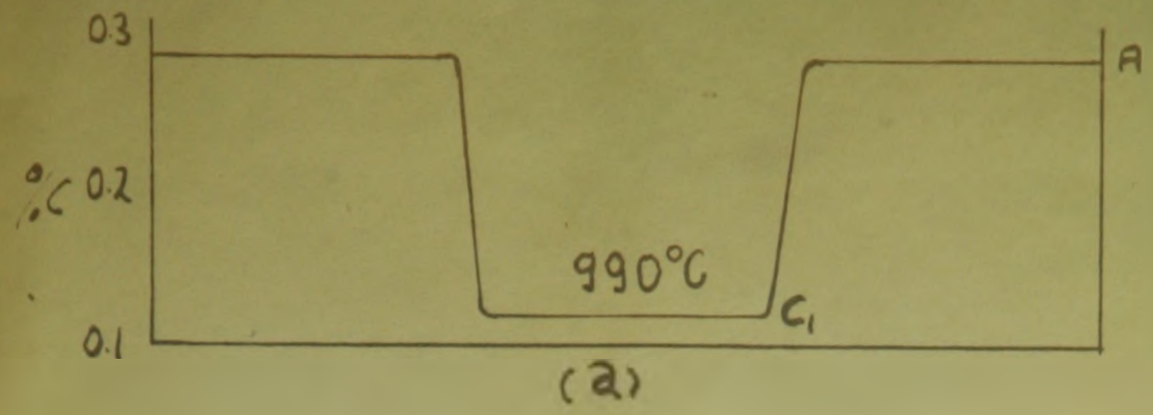

(a)

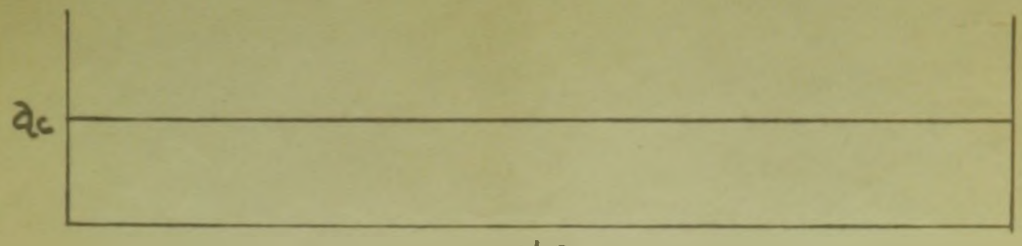

(b)

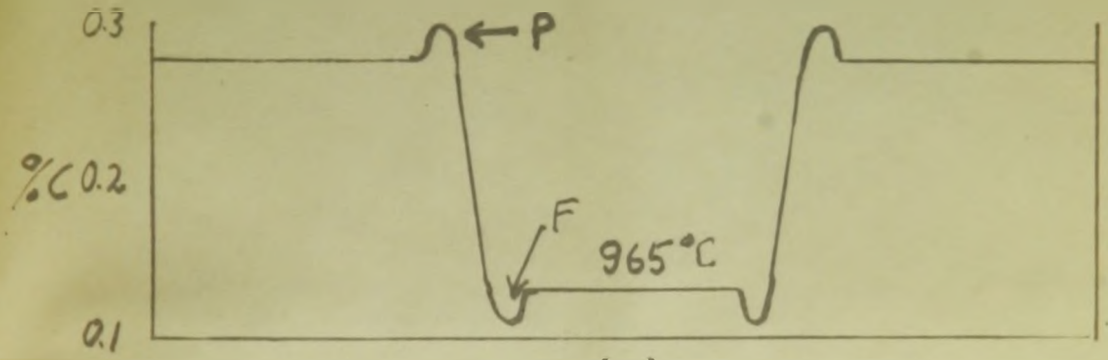

(c)

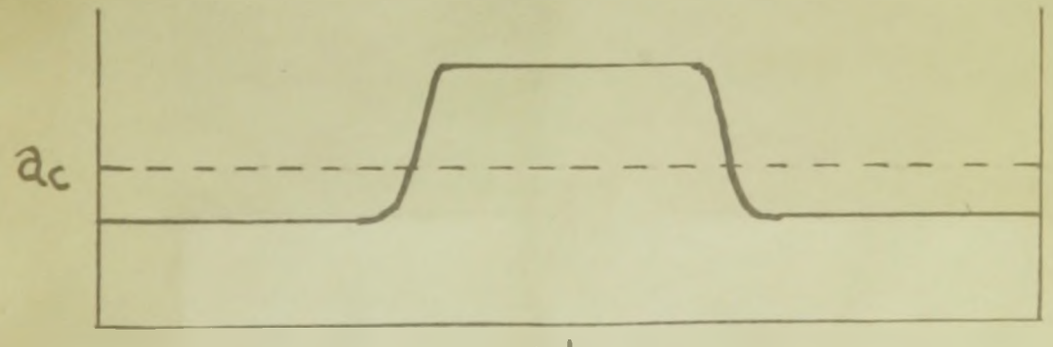

(d)

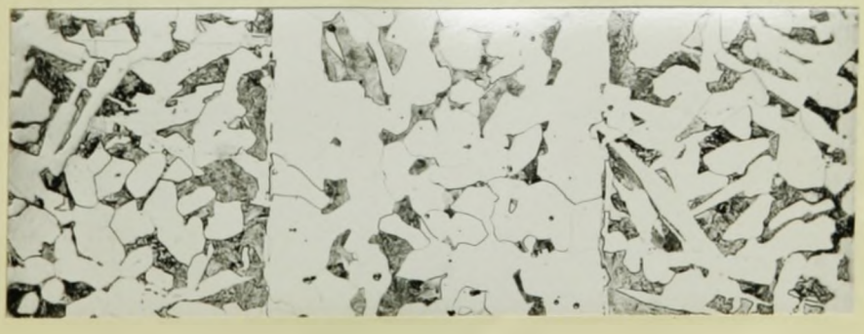

(e)

FIG. 19. Compositional and structural evolution of Fe-Si-C couple during very slow cooling.

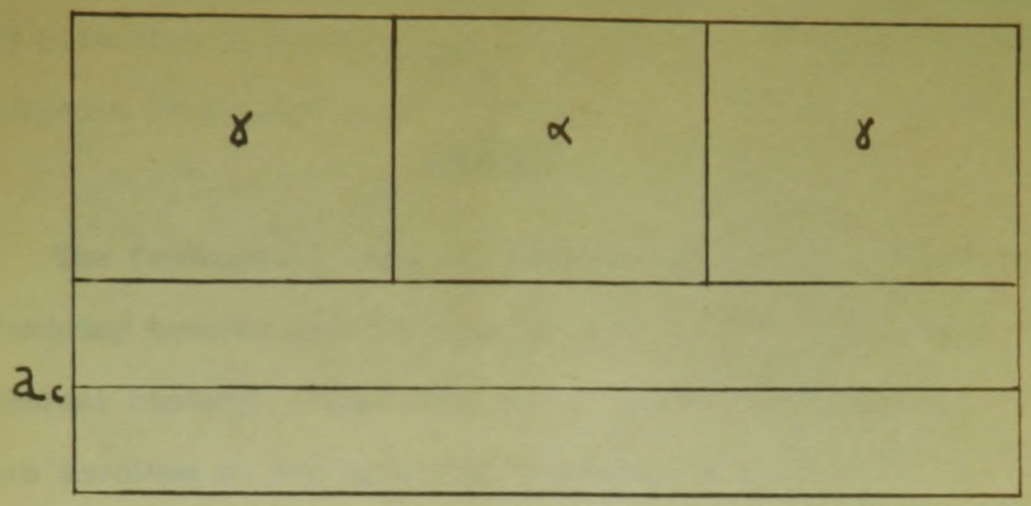

(a)

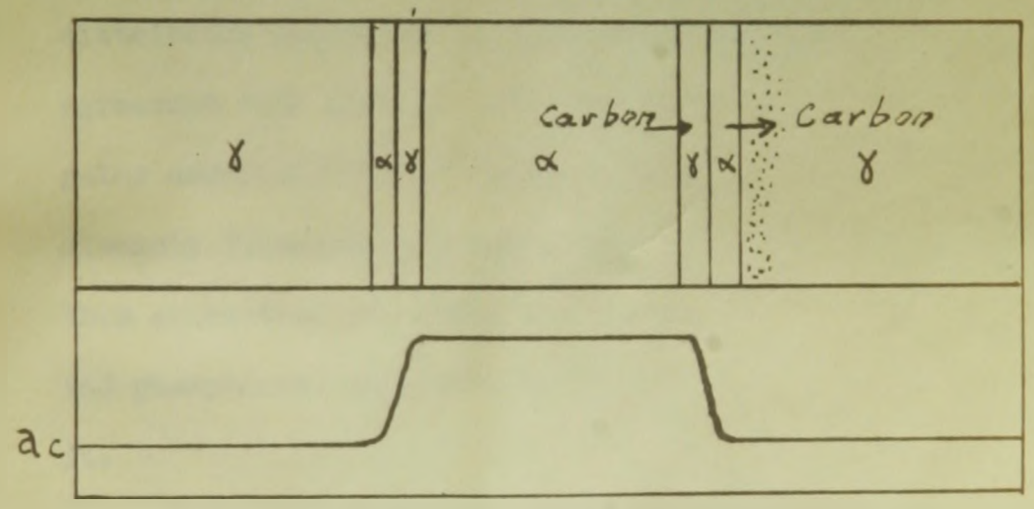

(b)

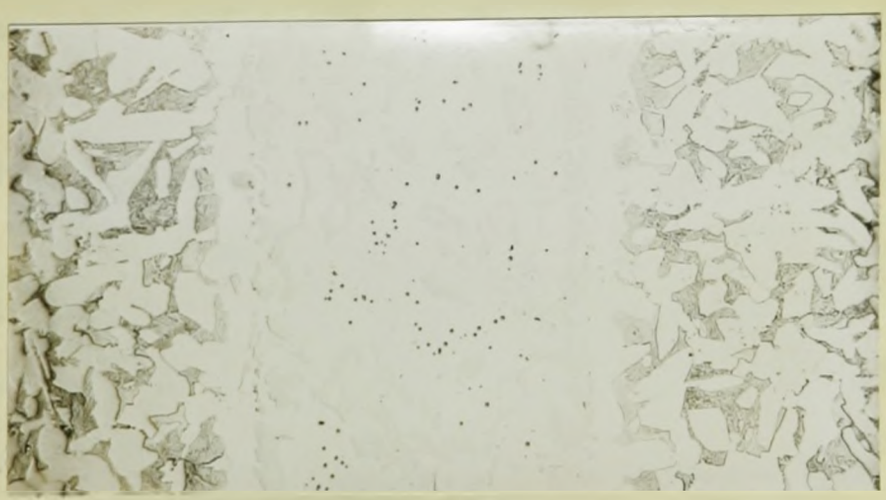

(c)

Fig. 20. Evolution of microstructure of the 0.9 phosphorous diffusion couple.

IV

SUMMARY

The fundamental cause of carbon banding in the steels studied is the tendency towards equalization of carbon activities at all stages of the thermal history. This primary cause can be broken down into specific factors involved at the different temperatures and transformation times.

a) At soaking temperatures, in the austenitic range, carbon distributes itself to equalize its activities as demonstrated in agreement with Bastien[7] and Jatczak et al[5]. The carbon segregates according to the experimental rule that carbide forming elements (chromium and manganese) lower the activity of carbon thus attracting it, while the solution type elements (silicon and phosphorus) increase the activity of carbon, thus repelling it.

b) On decreasing the temperature towards the A_3 line the presegregation of (a) tends to increase. This increase accounts in part for the strong directional bias of carbon flow which occurs during the subsequent intense segregation.

c) The factor which makes the largest contribution to the intensity of banding is that associated with preferential nucleation. The alloy segregated areas raise or lower the A_3 line causing ferrite nucleation to occur preferentially in one area or the other. This preferential nucleation is accentuated by the carbon presegregation.

The considerations brought forth in (b) and (c) did not receive proper attention in the previous literature and represent an original contribution to metallurgical science.

REFERENCES

1. Lavender, J.D., and F.W. Jones. An Investigation on Banding: The Journal of the Iron & Steel Institute, Volume 3, pp. 14-17, 1949.

2. Wolfe, K.J.B. Journal of the Iron & Steel Institute 160, September 1948, p. 31.

3. Betteridge, W., and R.S. Sharpe. Journal of the Iron & Steel Institute I, 1946, p. 217.

4. Schwartzbart, H. Effect of Manganese Banding on Mechanical Properties of Heat Treated Steel Plate in the Thickness Direction. Transactions of the A.S.M. 44 pp. 845-852, 1952.

5. Jatczak, C.F., D.J. Girardi and E.S. Rowland. On Banding in Steel: Transactions of the A.S.M. 48, pp. 279-305, 1956.

6. Plöckinger, E., and A. Randak. Untersuchung über das Zeilengefuge in unlegierten und legierten Baustahlen: Stahl und Eisen, 78, XV, pp. 1041-1048, 1958.

7. Bastien, P.G. The Mechanism of formation of Banded Structures. Journal of the Iron and Steel Institute, Volume 187, pp. 281-291, December, 1957.

8. Grossmann, M. Trans. Amer. Inst. Min. Met. Eng., 150, pp. 296, 1942.

9. Hayes, A., and J. Chipman. Trans. A.I.M.E., Volume 200, p. 85, 1939.

10. Chipman, J. Chap. 16 in "Basic Open Hearth Steelmaking" 1951, New York, Amer. Inst. Min. Met. Eng.

11. Darken, L.S. Diffusion of Carbon in Austenite with a Discontinuety in Composition: A.I.M.E. Transactions 180, pp. 14-17, September 1949.

12. Wells, C., and R.F. Mehl. Rate of Diffusion of Carbon in Austenite, in Plain Carbon, in Nickel, and in Manganese Steels: Transactions Am. Inst. Min. Met. Div. 1940, pp. 279-306.

13. Ham, J.L., R.M. Parke and A.J. Renrig. The Effect of Molybdenum on the Rate of Diffusion of Carbon in Austenite. Transactions of the A.S.M. 33, pp. 481-492. 1944.

14. Fick, A. Über Diffusion, Pogg. Am., 94, 1855, pp. 59.

15. Onsager, L. Ann. N.Y. Acad. Sci. 46, 1945-46, pp. 241.

16. Kirkaldy, J.S. Private Communication.

17. Kirkaldy, J.S. Diffusion in Multicomponent Metallic Systems # IV. Can. Jour. of Physics, 37, (1959), p.30.

18. Kirkaldy, J.S. Can. Jour. of Physics, 36, 899, 1958.

19. Smith, R.P. Jour. Am. Chem. Soc. 68, 1946, pp. 1163.

20. Smith, R.P., and L.S. Darken. Journal Am. Chem. Soc., 70, 1948, pp. 2724.

21. A.S.M. Metals Handbook.